

Intensity distribution conversion from Gaussian to Top-Hat in a single-mode fiber connector

Comparative study of optical simulation software FRED and ZEMAX

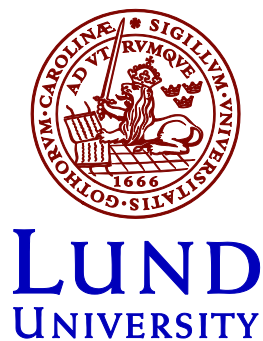
Master's thesis

Ola Willstrand

2013-01-25

Supervisors: Per Olof Hedekvist, SP Technical Research Institute of Sweden
Johan Mauritsson, Lund University

Examinator: Hans Lundberg, Lund University



Abstract

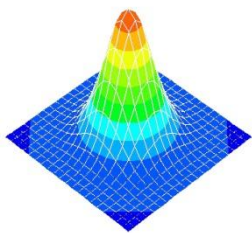
Gaussian to top-hat beam shaping is widely used today in areas of cutting, welding, and laser patterning. Typically, single-mode solid state lasers are used whose Gaussian intensity distribution is transformed into a top-hat. In this thesis the transformation is applied in a single-mode fiber connector, where the aim is a uniform intensity distribution of the emerging light from the connector. This is desirable in unclean environments where the probability of dirt or dust particles on the connector interface is high. Different methods of the transformation are analyzed, and the circular symmetric Powell lens is found most suited for implementation in a fiber connector. Two different connector-models where the Powell lens is involved are designed and for this purpose two optical simulation software products, FRED and ZEMAX, are used. These two products are compared concerning user friendliness, support, optimization feature, and accuracy of the simulations. The comparison is valid for the content of this thesis, but the scope of applications of these products reach far beyond this project. Because of the expensiveness in producing just one custom made lens, such as the circular symmetric Powell lens, instead cylindrical Powell lenses were used in the experiments, which are catalogue lenses. The experiments showed *i.a.* that the transformation predicted was successful. They also revealed some shortcomings in the simulation tools.

Keywords: Gaussian beam, top-hat, fiber connector, Powell lens, FRED, ZEMAX

Populärvetenskaplig sammanfattning

Det finns huvudsakligen två olika sätt att koppla ihop optiska fibrer. Det ena sättet är att föra fiberändarna direkt mot varandra och det andra sättet är att först kollimera ljuset (dvs. ljusstrålarna görs parallella) med t.ex. en lins efter fiberändan och sedan fokuseras ljuset ner i den andra fibern med hjälp av ytterligare en lins. I det senare fallet kan man låta ljusstrålen expandera innan kollimeringen så att strålen som kommer ut från kontakten har större diameter. Detta är en fördel i smutsiga miljöer eftersom ett dammkorn eller andra smutspartiklar på linsen har mindre inverkan om ljuset är utspritt över en större yta. Om single-mode fiber används kommer ljusintensitetsfördelningen i kontakten att vara Gaussisk, dvs. ljusstrålen har högst intensitet i mitten och avtagande intensitet utåt i radiell riktning. Detta innebär att t.ex. ett dammkorn på mitten av linsen dämpar mycket mer än om det är placerat längre ut. Det är därför önskvärt att istället ha en jämn intensitetsfördelning i ljusstrålen.

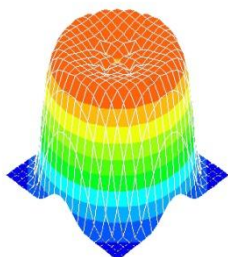
I denna rapport undersöks därför möjligheterna att transformera ljusintensitetsprofilen i en fiberkontakt. Utrymmet är begränsat i en fiberkontakt och det ställs höga krav på omvandlingseffekten. I rapporten anses Powell-linsen bäst lämpad för transformationen och tillsammans med konventionella sfäriska linser är två modeller framtagna. Modellerna simuleras i de optiska simuleringsprogrammen FRED och ZEMAX som sedan jämförs mot varandra med avseende på användarvänlighet, prestanda, tillförlitlighet m.m. I figur 1 visas den Gaussiska intensitetsfördelning ljusstrålen har när den lämnar fibern och i figur 2 ses ljusstrålens top-hat profil efter att den bl.a. passerat Powell-linsen. Bilderna är hämtade från simuleringar i FRED.



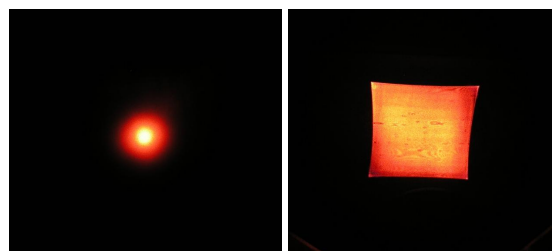
Figur 1. Gaussisk intensitetsprofil simulerad i FRED.

I simuleringarna används cirkulära symmetriska Powell-linser som måste specialbeställas. I experimenten används därför istället cylindriska Powell-linser som finns i vissa standardsortiment. Dessa genererar en rektangulär top-hat som kan ses i figur 3, där en He-Ne laser belyser en skärm med respektive utan Powell-linser mellan.

Slutsatserna är att transformationen är genomförbar, kopplingseffekten försämras inte nämnvärt, men kontakten blir något känsligare.



Figur 2. Top-hat profil genererad av Powell-lins i FRED



Figur 3. Laserbelyst skärm utan (vänster) respektive med (höger) cylindriska Powell-linser mellan.

Contents

| | | |
|-------|--|----|
| 1 | Introduction | 9 |
| 1.1 | Outline | 9 |
| 2 | Background | 11 |
| 2.1 | Gaussian to Top-Hat transformation | 11 |
| 2.2 | Optical simulation software products..... | 13 |
| 3 | Theory..... | 15 |
| 3.1 | The Gaussian beam..... | 15 |
| 3.2 | Single-mode fiber | 16 |
| 3.2.1 | Numerical Aperture..... | 16 |
| 3.2.2 | Fiber V-parameter..... | 17 |
| 3.3 | Lenses..... | 18 |
| 3.3.1 | Aberrations | 19 |
| 3.3.2 | Aspherical lenses..... | 20 |
| 3.3.3 | Anti-Reflection coating..... | 21 |
| 3.4 | Ray Tracing | 21 |
| 4 | Lens producers | 23 |
| 5 | Simulations | 25 |
| 5.1 | Simulation results | 26 |
| 5.1.1 | Top-hat profiles..... | 29 |
| 5.1.2 | Coupling efficiencies | 35 |
| 5.1.3 | Tolerances | 36 |
| 5.2 | Adjusted simulations for experiments..... | 40 |
| 6 | Experimental results..... | 43 |
| 7 | Comparison of optical simulation software FRED and ZEMAX | 47 |
| 8 | Conclusions..... | 49 |
| 9 | Acknowledgments..... | 50 |
| | References..... | 51 |

1 Introduction

The expanding beam technology is used in optical fiber connectors to reduce sensitivity to dust particles and other kinds of contamination. The expanded beam is also less sensitive to the effect of lateral and axial misalignment [1]. To build such a connector the easiest way to go is to put a spherical lens in front of the fiber end to collimate the expanding beam emerging from the fiber. An identical lens could then be used to refocus the beam into the next fiber, see Figure 1.

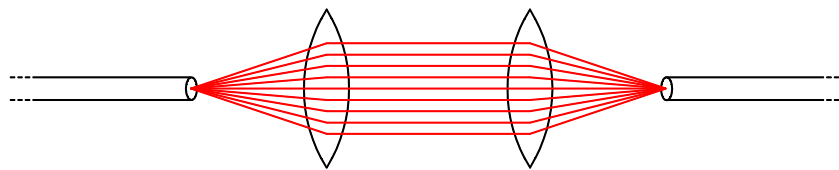


Figure 1. Illustration of an expanding beam fiber connector.

If this kind of connector is used with a single mode fiber, the expanded beam will have a Gaussian intensity profile in the radial direction. This means that if *e.g.* a dust particle is located on the center of the lens the attenuation will be greater than if the same particle is located further out. It is desirable to have equal attenuation regardless of the particle's location on the lens surface. In unclean environments, where the probability of dirt or dust particles on the connector is high, it would be preferable to have a uniform intensity distribution of the light. The aim of this diploma project is to design and construct an expanded beam single mode fiber connector, which transforms the beam intensity profile into a top-hat, *i.e.* a rectangular profile.

The project is done in cooperation with SP Technical Research Institute of Sweden AB. SP administrates the project and a major part of the work is located to SP's facilities in Borås. SP's interests lies in knowledge and experience more than in the product itself, but also in the analysis of different software products for optical simulations. Lund University uses a software product named FRED by Photon Engineering and SP uses ZEMAX by Radiant Zemax. A comparison and an analysis of the two simulation programs are, because of that, incorporated in the thesis.

1.1 Outline

The first two chapters of this thesis provide some background information and prior research on the topic. The historical methods of transforming a Gaussian beam into a beam with uniform intensity is presented and also a short discussion of previous comparisons of optical simulation programs.

In Chapter 3 the theory of some physical concepts and methods relevant for the thesis are explained. Those are the Gaussian beam, single mode fiber, ray tracing, and lens topics such as aberrations, coatings, and aspherical surfaces. After that some of the largest, or for this thesis most relevant, lens producers are introduced and presented. This since high quality standard lenses and also high precision custom made lenses are needed in the fiber connector.

In the following chapter the results from the simulations are presented, and in Chapter 6 the experimental results are provided. The report concludes with a comparison analysis of the two simulation programs and discussion of the results.

2 Background

2.1 Gaussian to Top-Hat transformation

Transformation of a Gaussian intensity profile into a uniform intensity profile of an optical beam has been a topic of research since the beginning of the 80's. Beams from many types of lasers take the form of a Gaussian beam and that is not always the most convenient shape for various applications, such as cutting, welding, and laser patterning. At high intensity the Gaussian profile could also damage optical components because of the intensity peak in the center. In these cases it is desirable with a uniform intensity profile, a top-hat. For transformation of a Gaussian beam into a top-hat there are many different methods, including truncation, beam combining, and methods based on reflection, refraction, or diffraction [2, 3]. In Figure 2 an illustration shows the conversion from a Gaussian intensity profile (Input) into a top-hat or uniform intensity profile (Output).

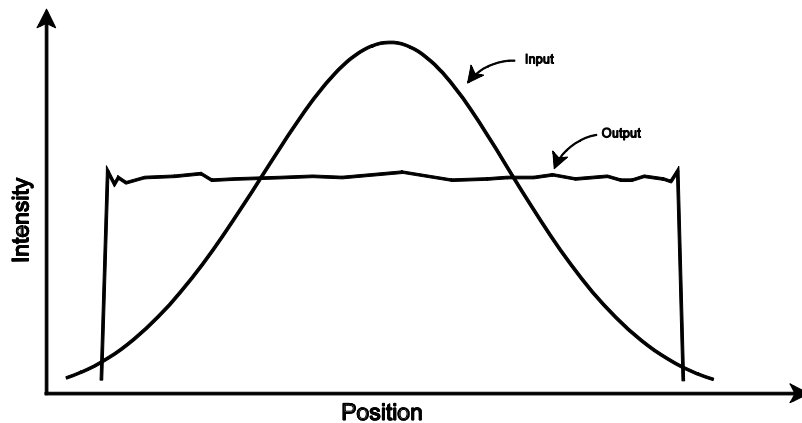


Figure 2. Illustration of Gaussian to top-hat conversion.

The easiest and probably the most frequently used way to perform this conversion is to truncate the Gaussian beam spatially using an aperture. This means that only the center part of the Gaussian beam, where it is almost flat, passes through. A similar approach is to use a filter with varying amplitude transmittance to flatten out the Gaussian beam. It is also possible to use a grating with varying diffraction efficiency [3], but common for these methods is that the conversion efficiency is very low because of the truncation.

To get higher conversion efficiency the irradiance has to be redistributed instead of truncated. In 1980 Rhodes and Shealy [2] presented and mathematically derived the concept of reshaping a collimated Gaussian beam into a collimated uniform intensity beam using two aspherical lenses. In this setup the first lens redistributes the intensity

and the second lens collimates the light rays again. The problem with this method, at that time, was that the fabrication of aspherical lenses was rather difficult. Instead a system of four spherical lenses that makes use of spherical aberrations [4] could be used to convert the beam, but compared to the system with two aspherical lenses the efficiency is lower. But fabrication of spherical lenses is easy.

In 1983 Han, Ishii and Murata [4] proposed using computer-generated holograms to create a new wave front. These could then replace the aspherical lenses in the system by Rhodes and Shealy. Since that paper a lot of different methods using holograms or various kinds of phase elements to manipulate the wave front have been developed [3, 5, 6]. These elements are easier to fabricate than aspherical lenses and it is easy to get different shapes of the uniform beam.

However, in the last decade the fabrication of aspherical lenses has accelerated. Today it is easy to order custom made aspherical lenses, and there are also two types of aspherical lenses that some manufacturers have in their standard range, axicons and Powell lenses, which are possible for Gaussian to top-hat conversion. In Figure 3 these two kinds of lenses are shown.



Figure 3. Photos of an axicon to the left and two Powell lenses to the right. [7, 8]

An axicon has a conical surface and is able to redistribute a Gaussian beam into a uniform intensity beam or a doughnut shaped beam [9, 10]. Already in 1983 this idea was conducted, but with a four side pyramid shaped lens to create a square top-hat [11]. The Powell lens is a cylindrical lens with a special shape such that a Gaussian beam stretches into a uniformly illuminated line. The (patented) approach is to place two Powell lenses after each other with the cylindrical axis at right angles, as in Figure 4 [12, 13]. Homburg and Mitra [14] also present a circular symmetric Powell lens to transform the Gaussian beam into a top-hat, but this lens does not occur in catalogues.

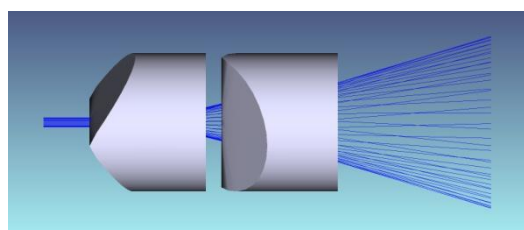


Figure 4. A combination of two Powell lenses to get a uniform intensity profile, simulated in ZEMAX.

An additional method of transforming a Gaussian beam into a beam with uniform intensity is to split up the beam and then recombine it in a more uniform pattern [15]. This method is relatively simple and especially suitable for very high power when the refractive optics will be damaged.

In this diploma project a refractive method is used due to demands on compactness and on high conversion efficiency. Since axicons and Powell lenses are included in some manufacturers' standard range, these formed a starting point for the continued work. An additional requirement in a fiber connector is that it is important that the transmitted beam is collimated, such that the inverse system could be used to refocus the beam into the next fiber. This is not the case of all methods described above as can be seen in Figure 4.

2.2 Optical simulation software products

There are various optical simulation software products on the market today and a lot has happened in the last decades regarding user friendliness and capacity. Not ages ago several optical engineers were needed just to run one simulation because of the complexity. Now it is much easier, and the programs have become greatly more powerful with complete packages of predefined objects, materials etc. and compatibility with other software products.

In this thesis a comparison between FRED and ZEMAX will be treated as mentioned in the introduction, but these two products are not alone on the market. In 2010 Linus Frantzich wrote a master's thesis at Lund University [16] including a comparison of optical simulation programs. He listed, according to him, the six most well known developers and their product, which are shown in Table 1. The products in the first three rows were said to be the most common and Frantzich choose to compare these three with FRED as a reference because of previous experience in that program. The result in that thesis was that Light Tools was preferred.

Table 1. Optical simulation software developers and their product.

| Company | Product |
|-------------------------------------|----------------|
| Optical Research Associates (ORA) | Light Tools |
| Breault Research Organization (BRO) | ASAP/APEX |
| Optis | OptisWorks |
| Photon Engineering | FRED |
| Radiant Zemax | ZEMAX |
| Integra | Specter |

However, there are many more products than this and about eighty different optical design software products are listed on Optenso's website [17].

The comparison in this thesis between FRED and ZEMAX will consider user friendliness, support or “help”-tool, optimization feature, correlation between simulation results and experimental results, and general opinion. It is important to realize that in many respects the evaluation will be subjective to the author of this report. Throughout the report pictures from the simulations will be alternate from FRED and ZEMAX to visualize the graphical interfaces.

3 Theory

3.1 The Gaussian beam

The Gaussian beam is an important solution to the paraxial Helmholtz equation, which originates from the wave equation. It describes a beam with circular symmetry and most of the beam power concentrated within a small cylinder along the beam axis. For a given beam width it is the Gaussian beam that exhibit the smallest angular divergence permitted by the wave equation [18]. The intensity $I(r, z)$ of a Gaussian beam depends on the radius r as

$$I(r, z) \propto \frac{1}{w^2(z)} e^{-\frac{2r^k}{w^2(z)}} \quad (1)$$

where $w^2(z)$ is a measure of the beam width and $k = 2$. Within a circle of radius $w(z)$ approximately 86% of the power is contained. If $k > 2$ the beam is referred to as super Gaussian and when k increases towards infinity the beam profile will transform towards a top-hat shape. The angular divergence θ of the beam is inversely proportional to the beam waist w_0 (Figure 5) as:

$$\theta \cong \frac{\lambda}{\pi w_0} \quad (2)$$

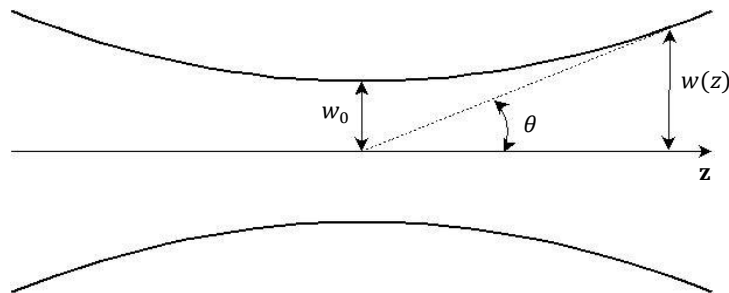


Figure 5. Gaussian beam width w as a function of the axial distance z .

3.2 Single-mode fiber

An optical fiber is a cylindrical dielectric waveguide and the theory of waveguides and in particular optical fibers may be studied more complete for example in *Fundamentals of Photonics* by Saleh and Teich [18]. In this section only the relevant concepts for this diploma work are considered, *i.e.* the mode profile of a single-mode fiber, the condition of single-mode, and numerical aperture.

Modes are eigenfunctions of the waveguide which mean that they maintain their shape along the waveguide axis. It is only the modes of the waveguide that can be guided. In a cylindrical optical fiber the modes' radial field distribution can be described by the family of Bessel functions and for the fundamental mode, which is the only mode propagating in a single-mode fiber, this is illustrated in Figure 6. In the figure $J_0(x)$ and $K_0(x)$ are the Bessel function of the first kind and the modified Bessel function of the second kind of zero order and a is the radius of the core. The fundamental mode is said to have a bell-shaped spatial distribution and the intensity distribution is very similar to that of the Gaussian beam. Therefore when the light emerges from the fiber it will take the form of a Gaussian beam. In comparison the beam from a multimode fiber will have a more uniform distribution due to the overlap of several different modes.

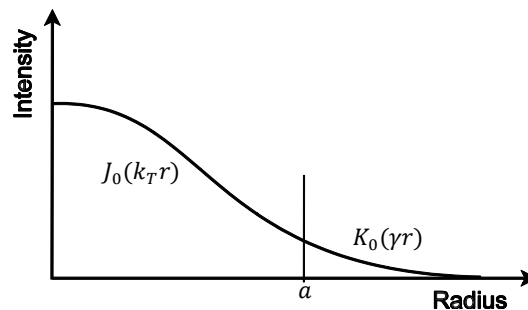


Figure 6. Radial field distribution of the fundamental mode in step-index fibers.

3.2.1 Numerical Aperture

The numerical aperture (NA) is an important parameter that defines the angular spread of light emerging from a fiber. It also defines the acceptance cone of what incoming light that can be guided due to total internal reflection in the fiber. However, in a single-mode fiber the incoming light also has to match the fundamental mode.

The numerical aperture for an arbitrary optical fiber is defined and related to the acceptance angle θ_a in Figure 7 as:

$$NA = n_s \sin \theta_a \quad (3)$$

where n_s is the index of refraction for the surrounding medium. For a step-index fiber the following equation can be derived from equation 3:

$$NA = \sqrt{n_{core}^2 - n_{cladding}^2} \quad (4)$$

This means that *e.g.* a small difference in refractive index between core and cladding results in a small numerical aperture and also a small acceptance angle.

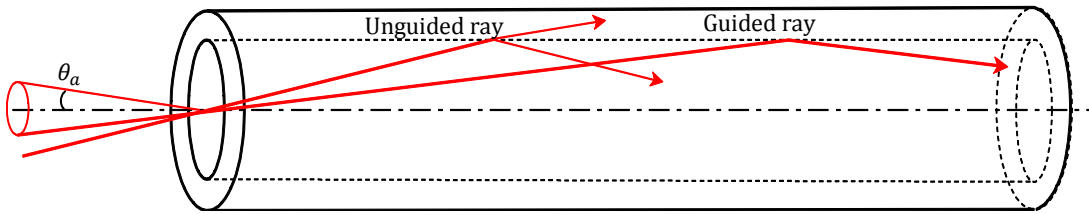


Figure 7. Illustration of the acceptance angle of an optical fiber.

3.2.2 Fiber V-parameter

The fiber V -parameter governs the number of modes in an optical fiber and is defined as

$$V = 2\pi \frac{a}{\lambda_0} NA \quad (5)$$

where a is the core radius and λ_0 is the vacuum wavelength. The parameter is just a convenient definition in the mathematical treatment and does not have a physical meaning, but is useful when determining the number of modes in an optical fiber. In particular the fiber is single-mode if $V < 2.405$, which is a table value that originates from a numerical computation [18, p. 336]. The wave equation cannot be solved analytically in an optical fiber. The single-mode restriction means that the fiber needs to have a small core radius, typically less than $5 \mu\text{m}$, and a small difference between refractive index, which gives a small NA .

3.3 Lenses

The object of a lens is to reshape the wave front impinging on the lens. This is simply achieved by the fact that the wave's speed depends on the medium it travels in. Hecht [19, pp. 150-153] shows mathematically that if a lens has a higher refractive index than the surrounding medium a hyperbolic surface will make the rays from a point source parallel, and an elliptical surface will perfectly focus incoming parallel rays. Although such surfaces would make lens systems very accurate, most lenses today have spherical surfaces. Traditionally, spherical lenses were the only lenses that could be made with high precision. This because of the unique property of spheres that two spherical surfaces of the same radius, one concave and the other convex, will perfectly match regardless of their orientation, see Figure 8. Both surfaces will then become more and more perfect spherical as they are polished against each other.



Figure 8. Photo of polishing a spherical lens [19].

If a hyperbolic or elliptical surface is replaced by a spherical surface the approximation is fairly crude far away from the central axis, but good close to it, see Figure 9. Of course there will occur image errors, called aberrations, but as long as the rays from a point source are almost paraxial the approximation is good. Furthermore, in well controlled spherical lens systems the aberrations can be made to counteract each other, so that the system becomes almost diffraction limited [19].

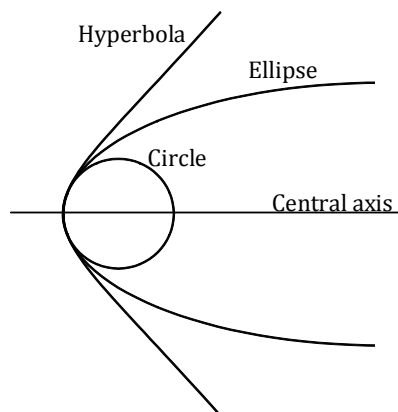


Figure 9. Illustration of a comparison between a hyperbola, an ellipse, and a circle.

3.3.1 Aberrations

There are two main types of aberrations: chromatic aberrations and monochromatic aberrations. Chromatic aberrations occur for all types of lenses and arise from the fact that the refractive index is a function of frequency. Monochromatic aberrations on the other hand depend on the shape and orientation of the lens. There are many different aberrations belonging to this group whereof spherical aberration, coma, astigmatism, Petzval field curvature, and distortion are the five primary aberrations. These are the most significant ones and are called the primary aberrations because they all arise from the first order approximation that $\sin \varphi = \varphi$, which is only a good approximation for very small values of φ (Figure 10). This approximation is implemented in the mathematical treatment when for example the Lensmaker's formula is derived, but is nothing else than that a spherical lens only is a good approximation in the paraxial region, i.e. when φ is small.

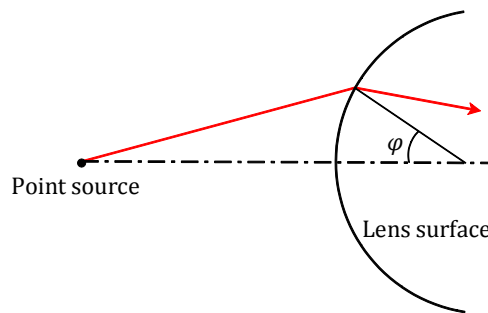


Figure 10. The definition of φ is the angle between the optical axis and the line between the spherical center of the lens and where the ray is incident.

Coma, astigmatism, Petzval field curvature, and distortion are all off axis phenomena and more information about these are available in *Optics* by Hecht [19]. However, in this report, since we are dealing with a fiber connector aligned along a single axis, only spherical aberration is significant.

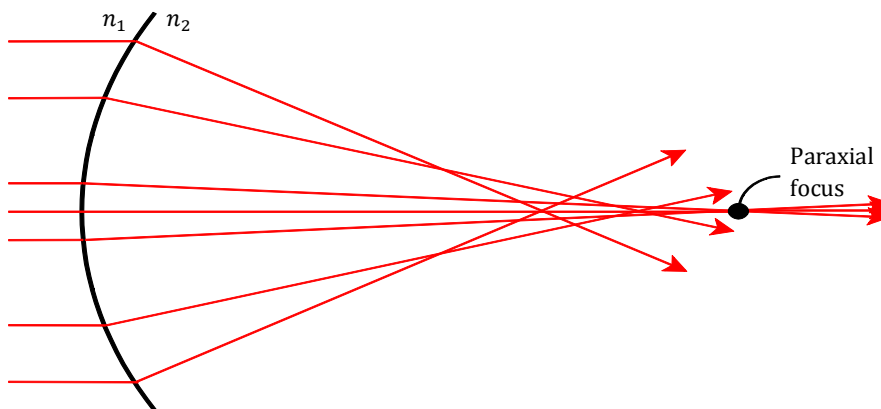


Figure 11. Illustration of spherical aberration.

Spherical aberration means that rays outside the paraxial region have other focuses than the paraxial ones, see Figure 11. As mentioned above, the surface has to be elliptical in this case to focus all rays to the same point. In an expanded beam fiber connector the most common is to use two spherical lenses, which result in that it is hard to get all light coupled into the next fiber due to spherical aberration. But this effect is possible to minimize, if *e.g.* plano-convex lenses are used the spherical aberration can be made smaller just by turning the lenses the right way, as is illustrated in Figure 12. Another way of reducing spherical aberration is to make doublets of one converging and one diverging lens [19].

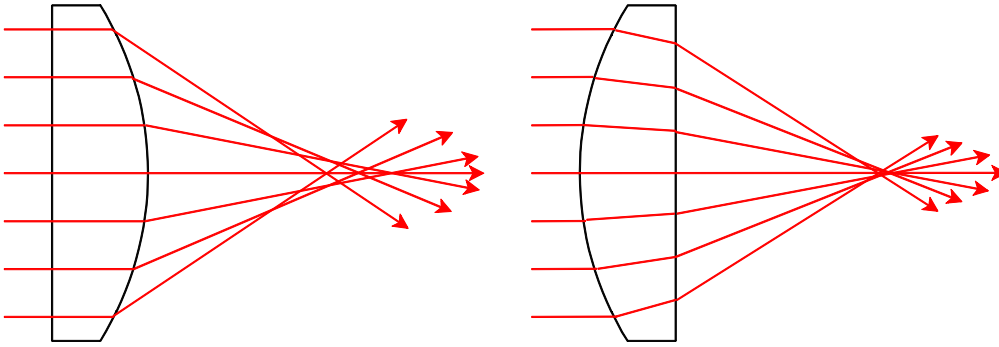


Figure 12. The amount of spherical aberration depends on the rotation of a plano-convex lens.

3.3.2 Aspherical lenses

Today it is possible to make high precision aspherical lenses, but they are still more expensive than the spherical. However, if better focus or almost aberration free systems are needed the aspherical lenses are an option. Aspherical lenses can also be used for beam shaping, as *e.g.* in converting a Gaussian beam into a top-hat. Standard aspherical surfaces are described by

$$z = \frac{cv * p^2}{1 + \sqrt{1 - cv^2(cc + 1)p^2}} + \sum_{i=2}^{\infty} A_i p^i \quad (6)$$

where z is a function of p , which is the radius in a circular symmetric situation and just x or y in a cylindrical case. If the conic constant, cc , is equal to zero and all polynomial terms, A_i , are also equal to zero, then the equation describes a spherical surface where the curvature, cv , equals the inverse lens radius [14].

For this thesis the surface of a Powell lens is of specific interest. It is described by equation 6, without polynomial terms and with the following constraints: [20]

$$\begin{aligned} cc &< -1 \\ 0.25 &< |cc * cv| < 50 \end{aligned} \quad (7)$$

3.3.3 Anti-Reflection coating

At the boundary between two media of different refractive indices there will be reflections according to the Fresnel equations. In particular between glass and air there will be about four percent losses due to reflections for light of normal incidence. In an expanded beam fiber connector with two glass lenses there are six glass-air boundaries, including the fiber ends, which gives about 22% in reflection losses. This value is for light of normal incidence, meaning that the real losses are probably even higher. To avoid such losses anti-reflection (AR) coatings can be used on the boundaries.

The simplest AR coating is just a thin film of refractive index n_2 between two media of refractive indices n_1 and n_3 . At normal incidence, the reflection at such an interface is zero if the thickness of the film is quarter of a wavelength and $n_2 = \sqrt{n_1 n_3}$. This is due to destructive interference between the reflection from the first boundary and reflections from the second boundary [18]. This AR coating is illustrated in Figure 13. To handle light that is not normal to the surface other kinds of multilayer AR coatings can be designed to reduce reflections.

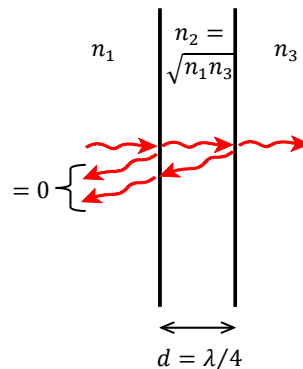


Figure 13. Anti-reflection coating ($\lambda = \lambda_0/n_2$).

3.4 Ray Tracing

The analysis of an optical system in optical simulation programs is based on ray tracing. Ray tracing means to follow the path of a light ray from its source to a detector. Describing light by rays that are perpendicular to the wave fronts, see Figure 14, is referred to as ray optics or geometrical optics. Ray optics is the limit of wave optics when the wavelength is very short compared to the system, and it is a very powerful approximation in optical system analysis. Moreover, in today's ray tracing programs, phase and polarization can often be added to the rays and, by calculating the optical path length, wave optics phenomena such as interference and diffraction can be included.

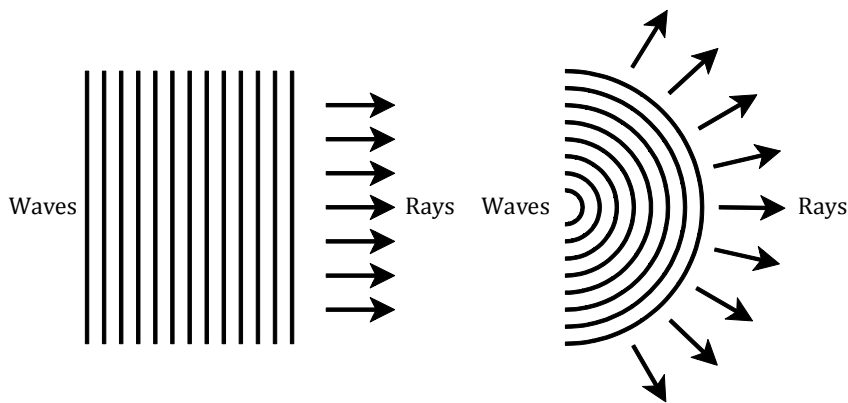


Figure 14. Two examples of rays (ray optics) compared to wave fronts (wave optics).

Ray tracing as a computer algorithm was first thought of in the early 1960s. This was in the field of computer graphics and the aim was to create photorealistic images. Unfortunately the computers back then were too slow and the images created were no good. As computers became more powerful the ray tracing algorithm was developed and improved. Ray tracing became one of the most powerful techniques in computer image rendering. With more powerful computers ray tracing was also implemented in optical design. In contrast to just create a photorealistic image the aim of optical design is to simulate the actual optical events. Even if both fields in principle can use the same ray tracing engine there is a main difference. Since the aim of computer graphics is to create a 2-D picture of a 3-D world it is only the rays that reaches the image plane that are of interest. These rays are probably just a little portion of all available rays and by tracing these rays backwards from the image plane to the source the work done by the engine will be substantially less than otherwise. This is called backward ray tracing. However, in optical design there is no presumption of the rays' paths and all rays have to be traced with the beginning at the source, which is called forward ray tracing. To see where the rays are going in the simulation program the rays have to be detected. The detector halts and counts the rays in each of its pixels and, taking into account the power scaling and wavelength, an analysis of the light can be done [21, 16].

4 Lens producers

There are several lens producers worldwide and these mentioned here are not claimed to be, without exception, the largest. Instead the selection is based on whose standard ranges that are available for insertion into FRED and ZEMAX.

- **Edmund Optics** is declared by themselves as a leading supplier of optics and optical components to industry and that they have been this since 1942 [22]. They also state to have the world's largest inventory of optical components. Their headquarters is located in the US, but they have regional offices in 16 other countries around the globe where the UK office serves Scandinavia.
- **CVI Melles Griot** declares themselves, since 1959, as a global leader in the design and manufacture of products that enable the practical application of light [23]. They have headquarters in the US and manufacturing and distributing facilities worldwide. The Nordic representative, Melles Griot AB, is located in Uppsala, Sweden.
- **JML Optical**, founded 1972, operates in the US and is specialized in custom optics. They design, manufacture and test precision optical assemblies, components and systems [24].
- **Newport Corporation**, established 1969, is declared by themselves as the world's premier source of photonics technology [25]. Especially their laser technology is world leading. They are headquartered in the US, but have 11 manufacturing facilities around the world. Newport Corporation includes leading brands such as Corion®, New Focus™, Oriel® Instruments, Richardson Gratings™ and Spectra-Physics®.
- **OptoSigma** is focused on thin film coatings, optical components, opto-mechanics and manual/motorized positioners. They emphasize to have the best products at the best prices along with the best service [26]. Located in the US they serve the Nordic countries by their authorized distributor von Gegerfelt Photonics in Germany.
- **Rolyn Optics** is a US company with manufacturing east of Los Angeles. They say about themselves to be the pioneer of quality optics distribution to industry and their experience goes all the way back to 1925 [27].
- **Thorlabs**, headquartered in the US, has design and production facilities in seven countries worldwide, whereof one in Sweden [28]. Thorlabs Sweden AB is located in Gothenburg and has extensive experience in design and manufacturing of optical systems. In total Thorlabs provides about 20 000 products.

These mentioned so far have, except Thorlabs, their standard ranges available for insertion into both FRED and ZEMAX. Thorlabs are available in ZEMAX and are presented above because of their large business in Sweden. In FRED there are no more standard ranges available, but in ZEMAX there are also those listed in Table 2. Of those is probably Asphericon of most interest, because aspherical lenses are used in the project. Asphericon is a relatively new manufacturer and expert of aspherical components established 2001 in Germany [29].

Table 2. Lens producers and country of their headquarters.

| Company | Country |
|-------------------------|-----------------|
| 3M Precision Optics | US |
| Anteryon | The Netherlands |
| Asphericon | Germany |
| Archer Optx | US |
| Befort Wetzlar | Germany |
| Comar | UK |
| Daheng Optics | China |
| DIAS Infrared | Germany |
| Diverse Optics | US |
| Ealing | US |
| ESCO | US |
| EKSMA Optics | Lithuania |
| GelTech Solutions | US |
| ISP Optics | US |
| LightPath Technologies | US |
| LIMO | Germany |
| Midwest Optical Systems | US |
| NSG America | US |
| Philips | The Netherlands |
| Qioptiq | Luxembourg |
| RPO | US |
| Ross Optical | US |
| Sigma Koki | Japan |
| Special Optics | US |

5 Simulations

In chapter 2.1 it was said that axicons and Powell lenses formed a starting point for the simulations. Axicons were rejected on an early stage since the rays from a Gaussian source passing the axicon seems to be impossible to collimate at the point where the intensity distribution is uniform, which is at point A in Figure 15. After this point the beam will become doughnut shaped. A Powell lens on the other hand will create a uniform distribution of the light far from the lens and not just at the intersection point where the rays are redirected. This makes it possible to collimate the beam as will be shown later.

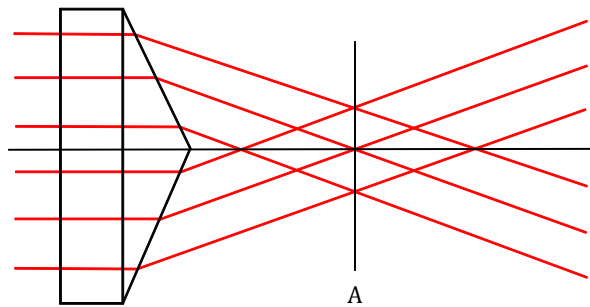


Figure 15. Illustration of rays passing an axicon.

The Powell lens is traditionally a cylindrical lens and, as was mentioned in chapter 2.1, two such lenses could be used to transform a Gaussian beam into a square top-hat. This approach is patented, but in this diploma project there is no need for a square top-hat and instead a circular symmetric Powell lens can be used to produce a circular top-hat. The benefit is that only one circular symmetric Powell lens is needed, which reduce the size of the system and losses due to reflections and absorption, which in turn are very important parameters in a fiber connector. Furthermore, rays from a circular symmetric Powell lens are much easier to collimate, because there is just one focus in contrast to when using two cylindrical lenses, which give different focuses in the x- and y-direction (though in strict sense a Powell lens does not have a well defined focus, but this will be shown later). The disadvantage is that the lens has to be custom made since it is only the cylindrical Powell lenses that occur in catalogues.

5.1 Simulation results

All simulations were performed in both FRED and ZEMAX. The simulations resulted in two different models, one where the beam from the fiber is collimated before the Powell lens and one where it is not. The first case, called model 1, is illustrated in Figure 16 with a picture from ZEMAX and the second case, called model 2, is illustrated in Figure 17 with a picture from FRED.

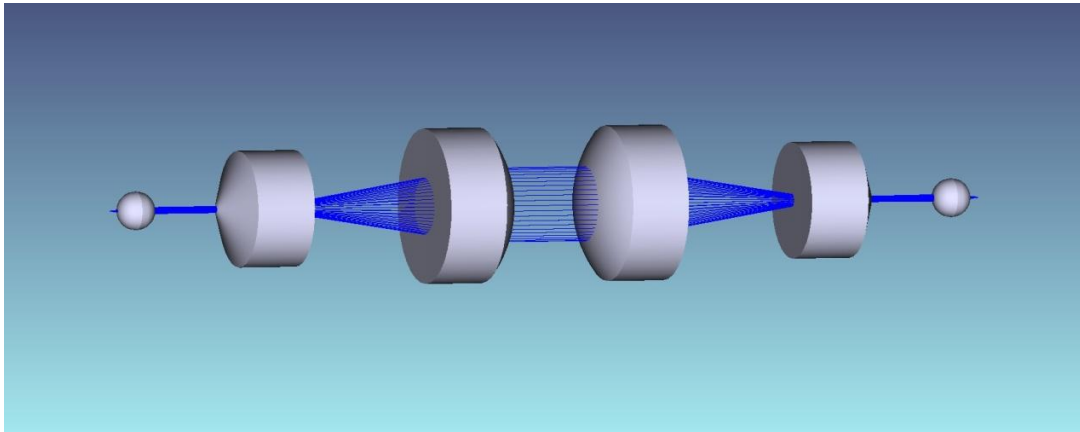


Figure 16. Model 1: Collimation before the Powell lens. Picture from ZEMAX.

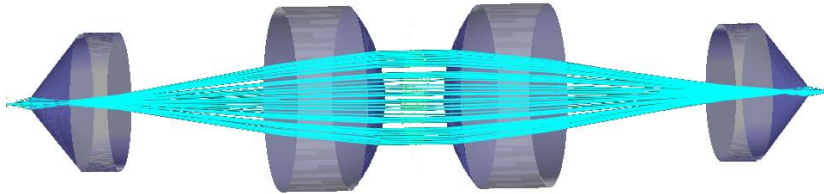


Figure 17. Model 2: No collimation before the Powell lens. Picture from FRED.

In the research on Gaussian to top-hat conversion the presumption has been a collimated beam to start with, so model 1 was the first one to be designed. In this model a ball lens collimates the beam emerging from the fiber tip and then the Powell lens redistributes the intensity and finally a standard plano-convex lens collimates the rays again. The inverse system is then used to refocus the light and couple it into the receiving fiber. The benefit of using a ball lens in the first position is that it is insensitive to rotations in the alignment procedure, but the curvature has to be large since the ball otherwise would become very big. This lens could, if preferable, be shaped different as long as it collimates the beam. The next lens in the system is the Powell lens, which is shown more clearly in Figure 18. Here you can actually see on the ray density that there is a Gaussian distribution before the lens and a uniform distribution after the lens. The

lens has gradually higher focusing power when approaching the center and what happens is that the high intensity in the middle comes to focus before the outer part of the beam. This means that the high intensity is smeared and overlaps with the lower intensity further out from the center when the beam diverges after the lens. It is also interesting to look at the positions spot diagrams before and after the Powell lens, Figure 19, where you can see how most of the rays are relocated to the outer region.

The idea behind the models in this thesis is that the beam approaching the Powell lens is narrow, such that the spatial difference between the two outermost focuses in the Powell lens is short. This means that from the plano-convex lens, where the beam is much wider, the rays seems to have a well defined focus in the Powell lens, which enables the use of a standard spherical lens to collimate the rays. Actually the spherical aberration of the plano-convex lens tends to counteract the focus splitting of the Powell lens.

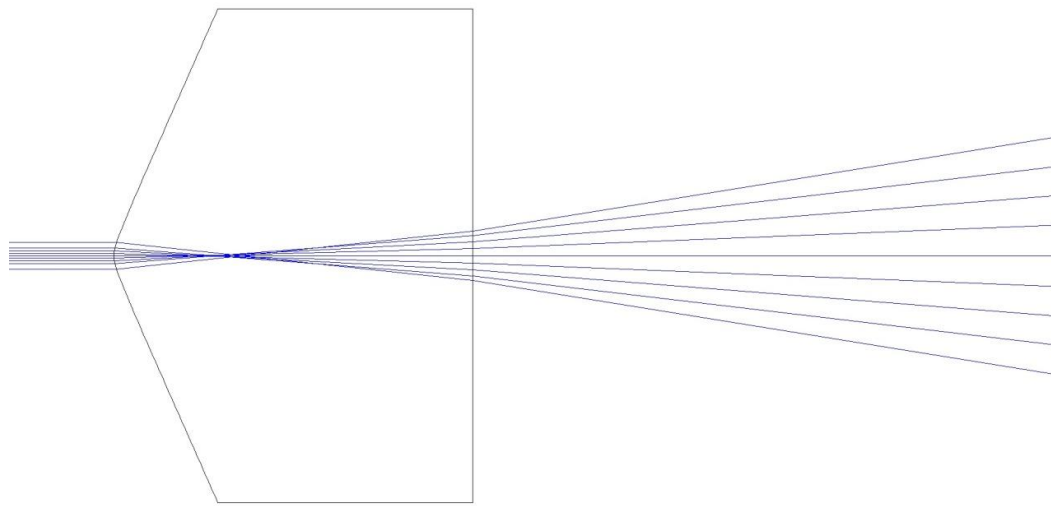


Figure 18. Powell lens (model1) simulation in ZEMAX. Gaussian to top-hat conversion.

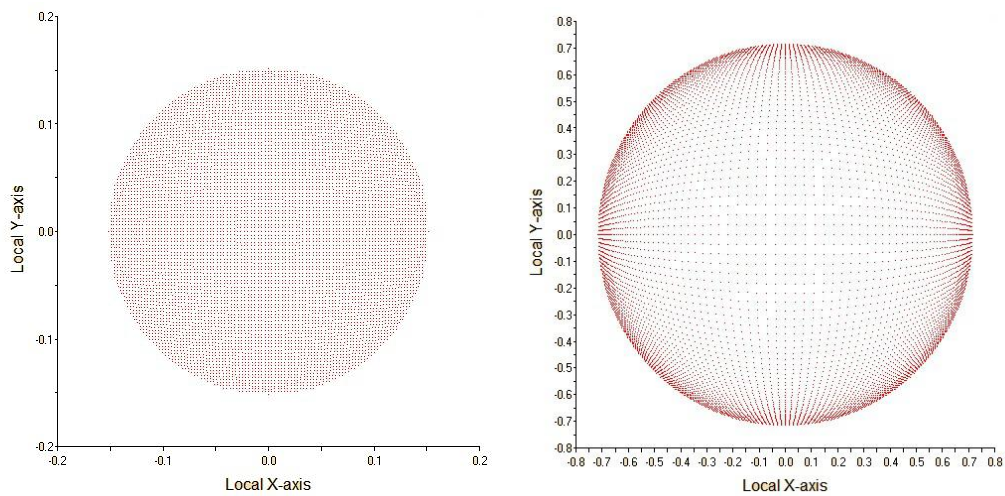


Figure 19. Positions spot diagrams before (left) and after (right) the Powell lens. Simulation in FRED.

In model 2 the idea is exactly the same as in model 1 except that the beam is not collimated before the Powell lens. Since the approaching beam now is diverging the parameters of the Powell lens have to be different to get an optimum top-hat profile. In Figure 16 and Figure 17 it is seen that the two Powell lenses are different. The fiber core, where the light originates from, has in these models a diameter of about 9 μm and the expanded beam is supposed to be about 2 mm in diameter. This dimension can be verified in the top-hat profiles presented in the next section.

All lens parameters for the two models are provided in Table 3 and all lenses, except the Powell lenses, are catalogue lenses from Edmund Optics. The parameters of the Powell lenses and the distances between lenses are optimized for a fiber $NA = 0.11$ and wavelength $\lambda = 1.31 \mu\text{m}$. All lenses have standard glass like Schott BK7 or equivalent. The conic constant and the curvature was introduced in equation 6, but to get a figurative understanding see Figure 20, where only the conic constant or the curvature vary between the different Powell lenses. Note that the conic constant has to be less than -1 to get the hyperbolic shape of the Powell lens.

Table 3. Lens specifications.

| | Curvature (mm^{-1}) | Diameter (mm) | Conic constant | Center thickness (mm) |
|-------------------|-----------------------------------|------------------|-------------------|--------------------------|
| Model 1 | | | | |
| Ball lens | 2.00 | 1.0 | - | 1.00 |
| Powell lens | 5.21 | 3.0 | -6.10 | 2.20 |
| Plano-Convex lens | 0.322 | 4.0 | - | 2.26 |
| Model 2 | | | | |
| Powell lens | 12.6 | 3.0 | -2.48 | 2.07 |
| Plano-Convex lens | 0.322 | 4.0 | - | 2.26 |

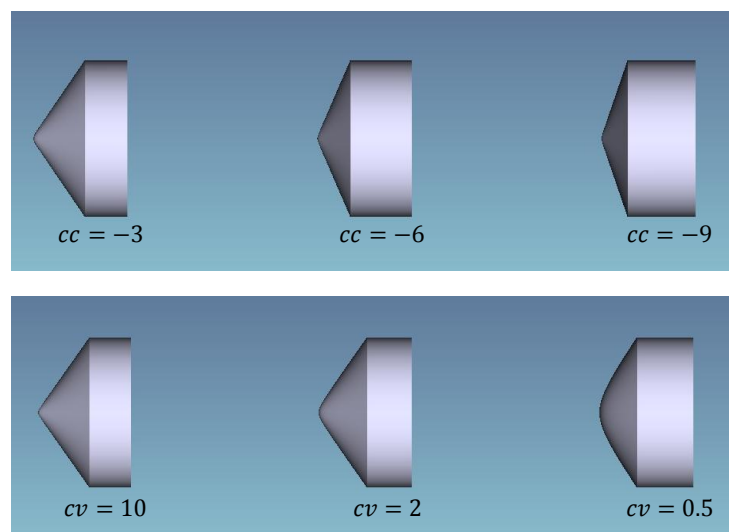


Figure 20. On top three Powell lenses with same parameters except conic constant and lowermost three Powell lenses with same parameters except curvature.

5.1.1 Top-hat profiles

The intensity profiles were measured midway between the two plano-convex lenses. Both simulation programs gave similar results except in one interesting case, namely when using *Physical Optics Propagation* on model 2 in ZEMAX. Both FRED and ZEMAX are based on ray tracing described earlier, which means that they primarily use ray optics or geometrical optics. But in this thesis also ZEMAX's analysis option *Physical Optics Propagation* (POP) is used. As mentioned in chapter 3.4, wave optics phenomena such as interference and diffraction can be included in ray tracing, but POP claims to be based on wave optics and the beam is represented by an array of discrete sampled points defining a wave propagating through space, instead of rays. This method is generally much slower than using ray optics and requires a quite large computer primary memory (RAM). There are three occasions though when POP is superior: when the beam comes to an intermediate focus, when analyzing diffraction effects far from focus, and at long propagation lengths when the beam is nearly collimated. Yet POP is not perfect and ZEMAX says that POP is generally not accurate for systems including non-sequential component groups [30]. In this project POP sometimes give similar results as when using ray optics and sometimes complete different results. When the results are different it is important to verify by experiments which method is most accurate and not just assume it is POP.

The results from the two models simulated in FRED and ZEMAX are illustrated in figures 21–26. Model 2 generates a more perfect top-hat when using ray optics, but when using POP large oscillations occurs. This reminds of Gibbs phenomenon [31] that originates from a discontinuity that cannot be described by Fourier series, and in Figure 23 one can see how the steep edges forms discontinuities. Unfortunately no experiments are done on this model to further analyze this effect for reasons that will be mentioned later.

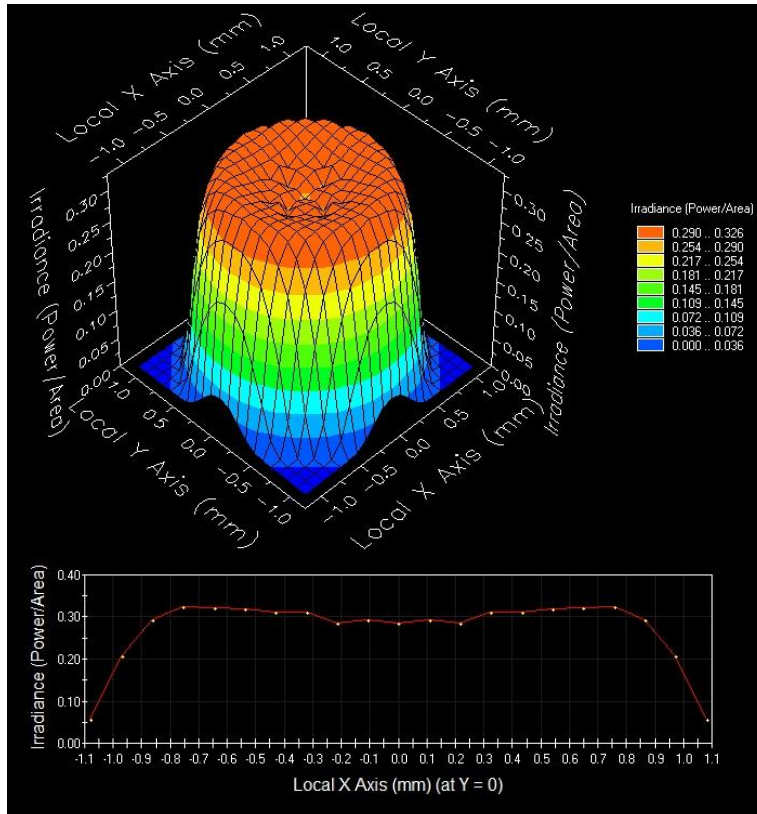


Figure 21. Top-hat profile from model 1 in FRED.

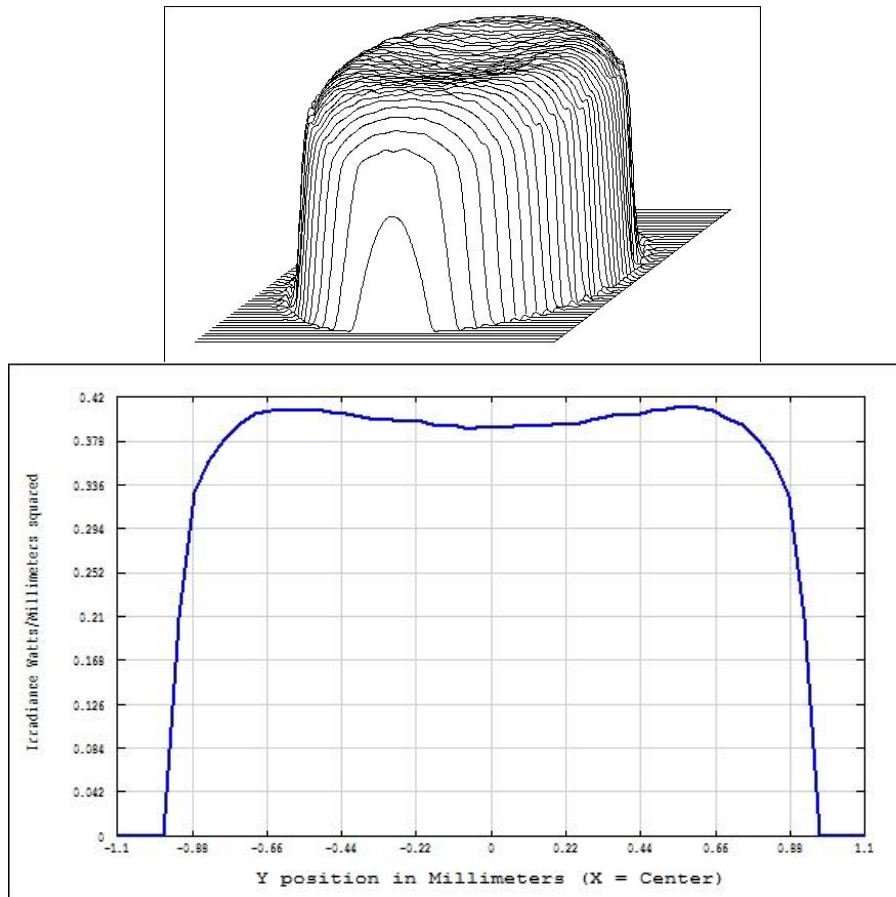


Figure 22. Top-hat profile from model 1 in ZEMAX.

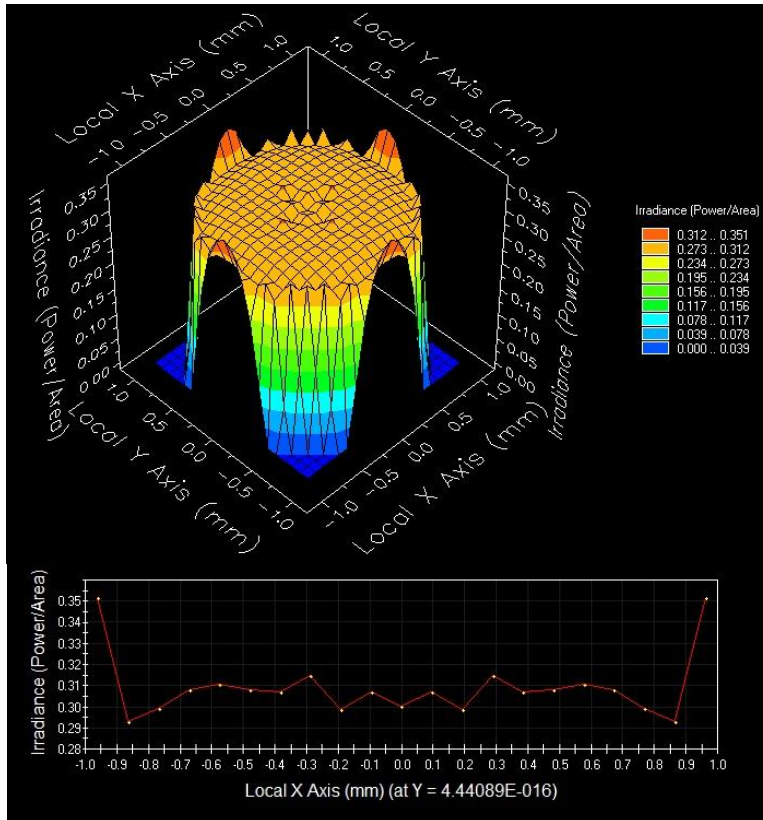


Figure 23. Top-hat profile from model 2 in FRED.

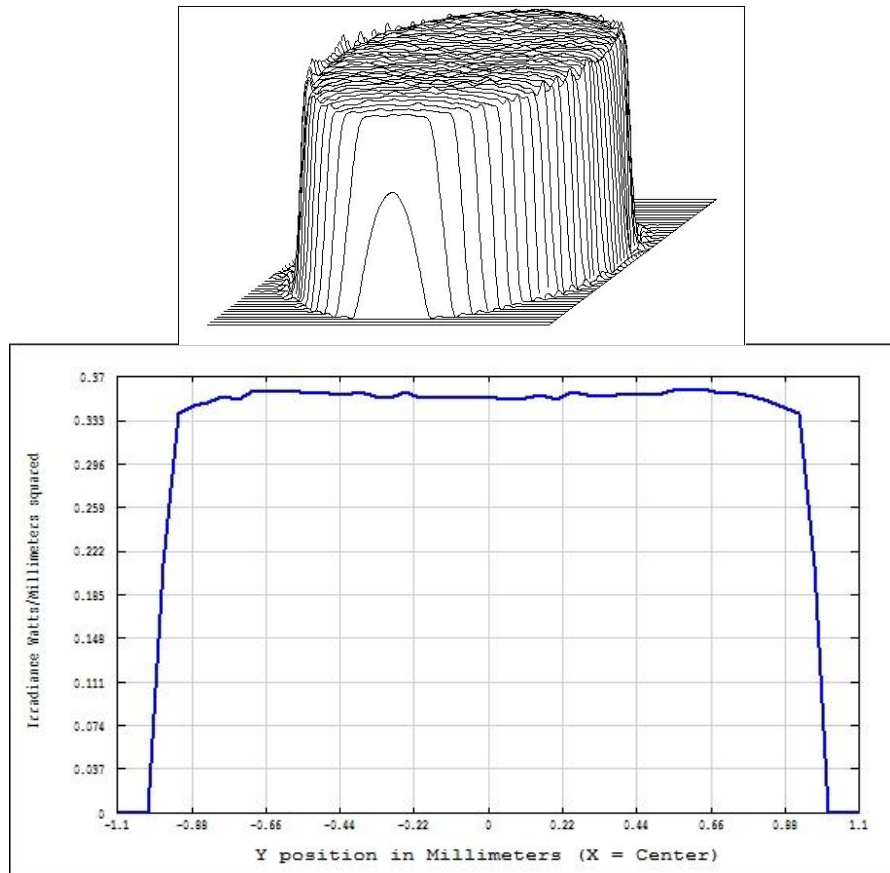


Figure 24. Top-hat profile from model 2 in ZEMAX.

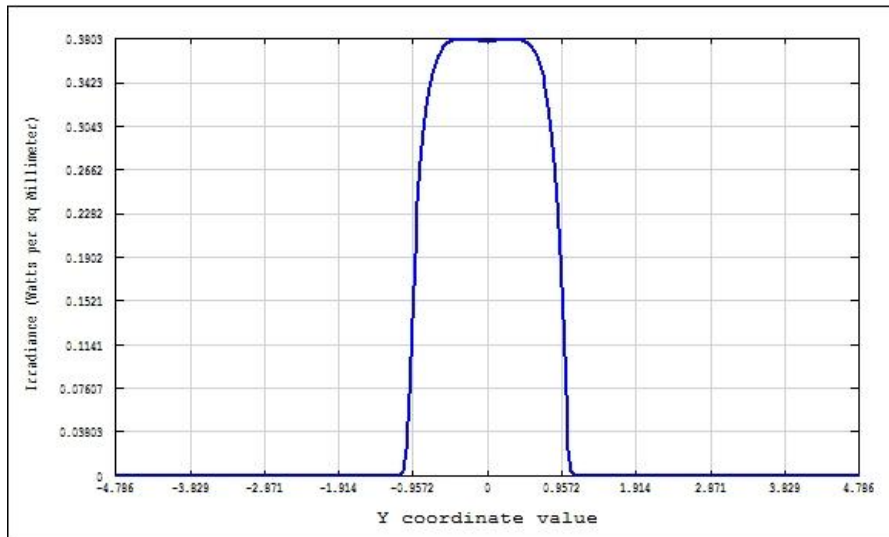


Figure 25. POP generated profile in model 1 in ZEMAX.

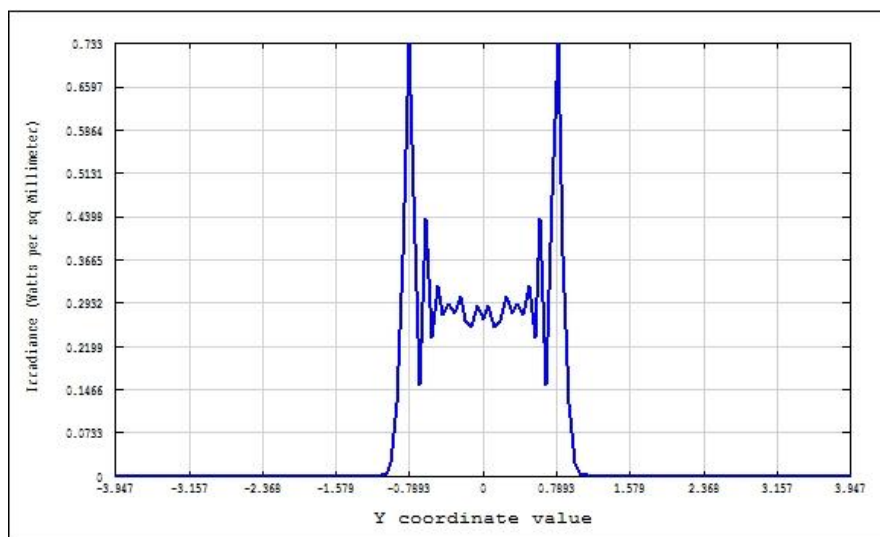


Figure 26. POP generated profile in model 2 in ZEMAX.

Simple expanded beam fiber connector

To compare the models to a standard expanded beam fiber connector a very simple model with just two plano-convex lenses, seen in Figure 27, was simulated. This model, called model 3, was primarily simulated to compare coupling efficiencies, but we can also look at the intensity profile in Figure 28 and see the difference between a Gaussian profile and a top-hat. Looking closely (compare *e.g.* figure 21 and 28) one can see that the maximum irradiance (same as for intensity) has dropped with almost 60% when having a top-hat instead of a Gaussian profile.

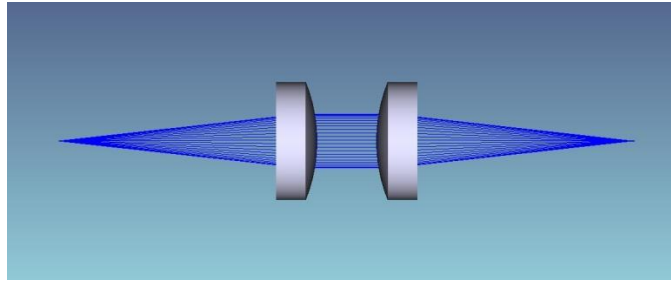


Figure 27. Model 3: Simple expanded beam fiber connector model.

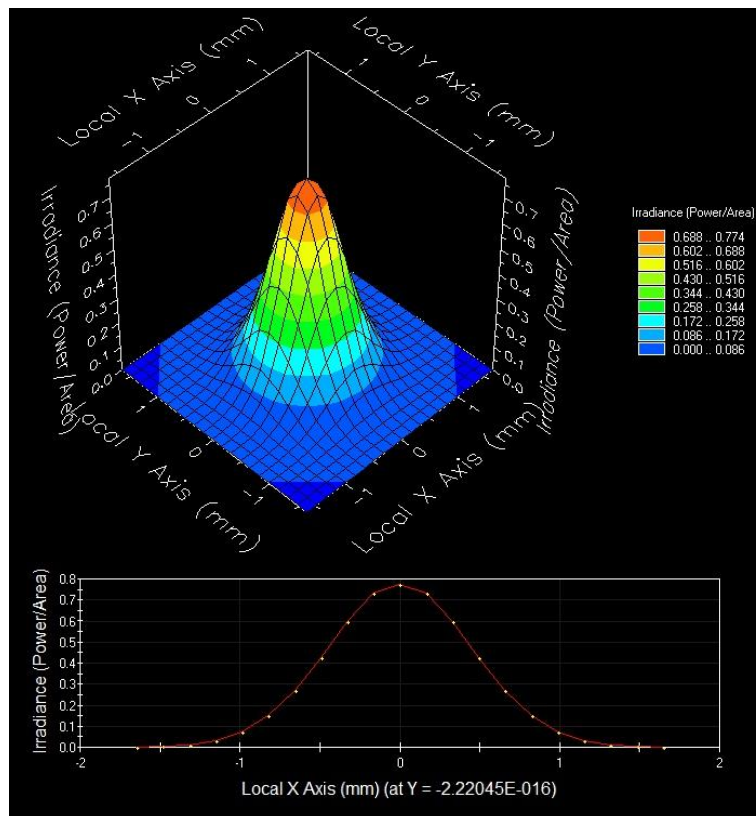


Figure 28. Gaussian profile from model 3 in FRED.

Manually optimized top-hats

Due to poor top-hat optimization algorithms the best top-hat profiles were generated manually. In FRED the built-in optimization feature was used to minimize peak-to-valley on the analyze surface, but there was a few considerations: first the analyze surface cannot be made circular, which means that the whole beam was not covered since if the surface extends outside the beam those low values will be included. Secondly to prevent the beam from locate itself outside the analyze surface like a doughnut the optimization had to include maximum power on the surface. The result was fairly good, but could be made better manually. After consulting the FRED support a knowledge base article was found which describes how to optimize for a target distribution [32]. For this project the

desired irradiance profile is just created from a uniform source profile and then a user-defined merit function aberration is the root mean square (RMS) difference between the real distribution and the target distribution. This optimization method could work, but the problem in FRED is that the rays cannot be analyzed without being halted, which means that you cannot analyze the intensity distribution in the middle of the model at the same time as analyzing the coupling efficiency at the receiving fiber. So, the optimization in FRED was focused on the coupling efficiency and the top-hat profiles were mainly optimized manually. It should though be said that there are, more or less complicated, ways around this problem, but that was realized too late to be examined in this project.

In ZEMAX rays can be analyzed without being halted and a macro (a script) for Gaussian to top-hat conversion, found in the ZEMAX knowledge base, was tested [33]. This macro defines a merit function, and the target is the conversion illustrated in Figure 29 with a given beam waist W and top-hat radius K . If the energy A equals the energy B a relation between the ray coordinates S and X can be derived:

$$S = K\sqrt{1 - e^{-2X^2/W^2}} \quad (8)$$

The macro was modified to fit into the models in this thesis and the result was again fairly good, but not sufficiently good. So, also in ZEMAX the best results were obtained manually. However, in ZEMAX there are a tool called “Slider” that is very effectively when adjusting manually. The Slider allows you to slide over an interval for a given parameter while continuously all open windows are updated. Further, more than one Slider can be used at the same time to adjust more than one parameter.

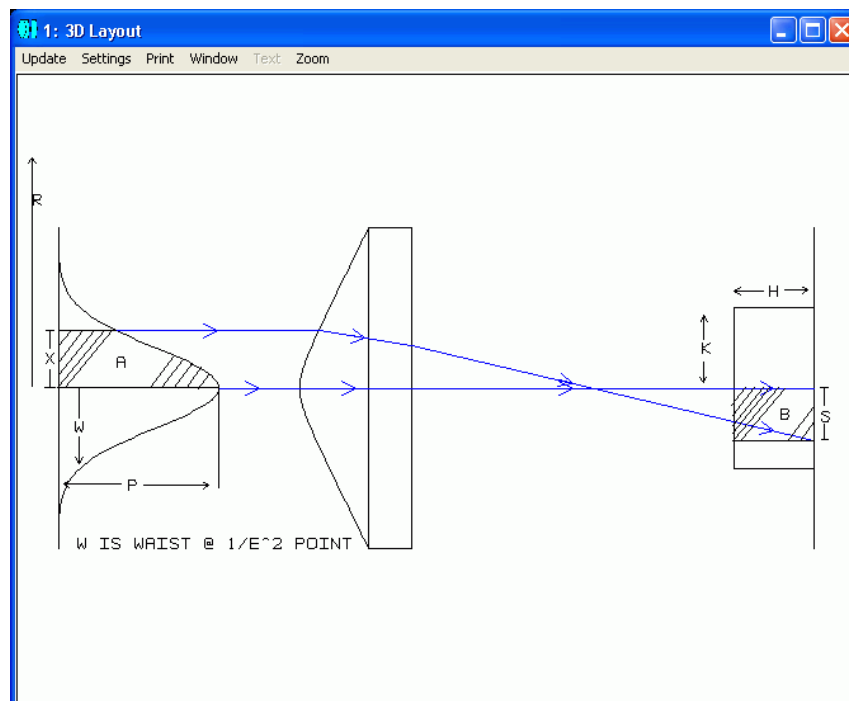


Figure 29. Conversion of a Gaussian profile with beam waist W to a top-hat profile with radius K . [33]

5.1.2 Coupling efficiencies

In optical fiber connectors a good coupling efficiency is vital. The highest coupling efficiencies achieved for the three models are presented in Table 4. The fiber $NA = 0.11$ and the core diameter is $9.14 \mu\text{m}$. The first three rows present ideal efficiencies with 100% transmittance through lenses and fiber ends and the last three rows show the real coupling efficiencies. The coatings are applied to all interfaces and the AR coating is a simple one layer coating explained earlier in this thesis and the HEAR1 coating is a more advanced multilayered coating.

Table 4. Coupling efficiencies (model 3 is the reference model in Figure 27). In the first three rows it is just the receiver efficiency, i.e. no losses due to reflections at the air-glass interfaces.

| | Model 1 | Model 2 | Model 3 |
|---------------------------|---------|---------|---------|
| FRED | 85.9% | 93.1% | 85.5% |
| ZEMAX (Ray optics) | 81.8% | 30.4% | 81.1% |
| ZEMAX (POP) | 82.5% | 86.3% | 80.8% |
| Uncoated (ZEMAX POP) | 51.6% | 63.5% | 67.0% |
| AR coating (ZEMAX POP) | 71.1% | 77.2% | 79.3% |
| HEAR1 coating (ZEMAX POP) | 81.8% | 79.3% | 78.1% |

The coupling efficiency for single mode fibers is generally calculated as an overlap integral between the wavefront mode at the fiber end and the fiber mode. However, in FRED there was an error message that this calculation could not be performed because the beam from the source must be coherent, but also when the beam was coherent the same error message popped up. Instead the coupling efficiency was calculated in FRED by measuring how much light that passed through the receiving fiber. This method is good when dealing with multimode fibers, but in a single mode fiber you have to consider how the light matches the fiber mode. This is probably why the efficiencies from FRED are slightly higher than the ones from ZEMAX.

Why the coupling efficiency in model 2 is so low when using ray optics in ZEMAX is puzzling. The losses come from the mode overlap integral, which is not calculated in FRED, but still the POP calculation is more consistent with the FRED result. Again it would have been interesting with some experiments on this model. But beside that value the efficiencies are at least as good as for the reference model, which is great. It is also interesting to look at the effects of the coatings. In model 3 the AR coating is sufficient, probably because the rays hit the interfaces fairly parallel to the normal. In model 1 the multilayered coating is needed, since the rays have larger incident angles to the interfaces. Also in model 2 the same effect is expected, but here the incident angles are even larger at the front surface of the Powell lens and maybe the HEAR1 coating is not enough to take care of the reflections.

5.1.3 Tolerances

The coupling efficiencies are generally very sensitive for defects and misalignments in the system. Regarding defects or imprecision in the surfaces of the lenses there are many parameters to consider, but the result presented here is mainly misalignments of the individual lenses or the receiver connection. In FRED a script was made to run through parameters continuously resulting in nice graphs. These are presented in Figure 31–32 and 34–36 and are discussed subsequently. In ZEMAX there is a tolerance feature that is particular powerful when analyzing how known manufacturing tolerances affect the system, but restricted to a determined aberration when analyzing tolerances. This means that a specific coupling efficiency was determined, in this case 70%, and then the tolerances were given that reduce the coupling efficiency to this value. The result is presented in Table 5 and all presented tolerances in this section reference to the ideal coupling efficiencies with no losses due to reflections. The two values in each box correspond to the first and second lens of same type in the connector and if only one value is present it is the same for both lenses. The available element tolerances in ZEMAX are tilt and decenter in the radial direction (Figure 30).

Table 5. Lens tolerances in ZEMAX for ray optics simulations and POP simulations. The tolerances apply to a decrease of the coupling efficiencies to 70%. In model 2, using ray optics, the ideal coupling efficiency is already below 70%, so these boxes are blank.

| | Decenter (mm) | Tilt (degrees) | Decenter POP (mm) | Tilt POP (degrees) |
|----------------|---------------|----------------|-------------------|--------------------|
| Model 1 | | | | |
| Ball lens | 0.0015 | 0.17, 0.18 | 0.0093, 0.17 | 1.1, 16.1 |
| Powell lens | 0.0009 | 0.07, 0.04 | 0.0033, 0.0030 | 0.24, 0.12 |
| P-CV lens | 0.0009 | 0.03, 0.07 | 0.0030 | 0.11, 0.25 |
| Model 2 | | | | |
| Powell lens | - | - | 0.0048, 0.0032 | 0.28, 0.13 |
| P-CV lens | - | - | 0.0032 | 0.12, 0.27 |
| Model 3 | | | | |
| P-CV lens | 0.0016 | 0.11, 0.17 | 0.28, 0.30 | 5.1, 4.5 |

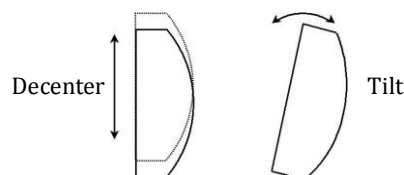


Figure 30. Decenter and tilt illustration.

The tolerances from ZEMAX are a bit confusing. First thing to notice is the big difference in the results from using POP instead of ray optics. Experimental results indicate that the tolerances based on ray optics are the most accurate ones, but it is puzzling that the difference in sensitivity between the top-hat models and the reference model is so large when using POP. The tilt occurs around the first surface and not around the center of the

lens, which explains why there are tilt tolerances at all for the ball lenses. It also explains the tilt values for the Powell lenses and the plano-convex (P-CV) lenses, which are lower when tilts are applied at the plane surface of the lenses. The curved surfaces are the important ones and when rotating around the plane surface both a tilt and a displacement take place at the curved surface, which lower the tolerance. At last also notice the high tolerances for the second ball lens when using POP, which is a bit strange.

In FRED there was a very small difference between tolerances of the two lenses of same type, so in Figure 31 and Figure 32 there is just one of each kind represented. If looking in Figure 31 at 70% coupling efficiency one can see that the tolerances are not far from what was obtained in ZEMAX using ray optics (column 1 in Table 5). Further, since the maximum coupling efficiencies were different in FRED and ZEMAX the values at 70% are not expected to be identical, but the ratio between the different lenses should be the same, which they are. In Figure 31 it is also interesting to see how there is an interval, except in model 2, where the coupling efficiency does not change at all.

Figure 32 is a little messier because there is no symmetry and the different lenses behave quite different. The asymmetry is interesting and means that the tolerances are very different depending in which direction the displacement occurs. But it should be noticed that the x-axis is different from Figure 31, so the system is much more sensitive for misalignments in the radial direction. Also notice in model 1 and model 3 how the coupling efficiency increases with a displacement in the right direction.

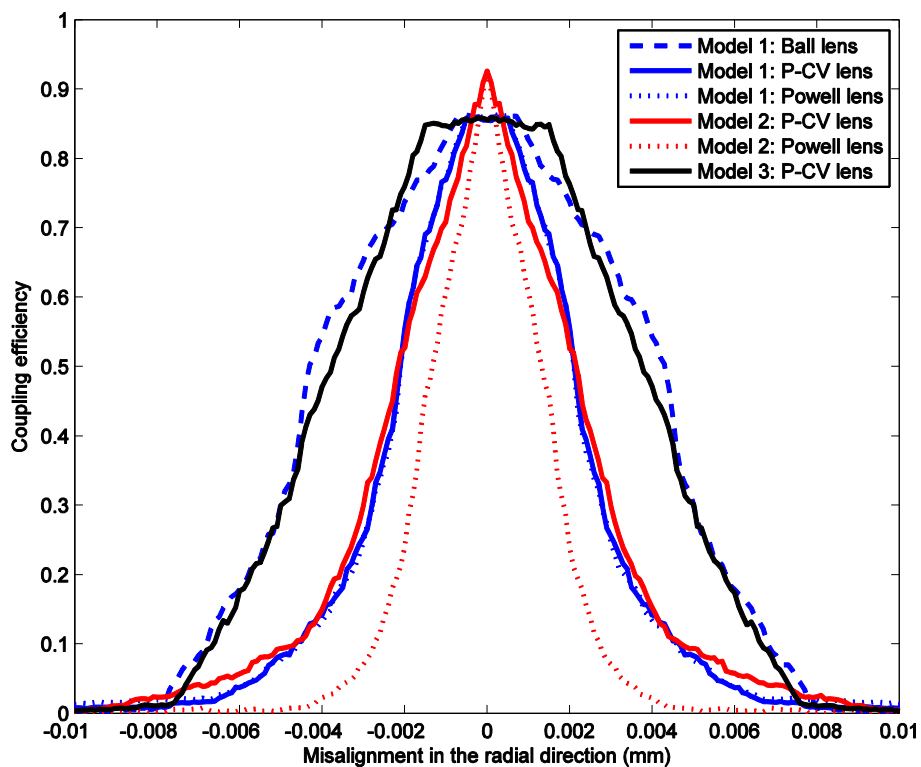


Figure 31. FRED tolerances for misalignment in the radial direction for all lenses separately.

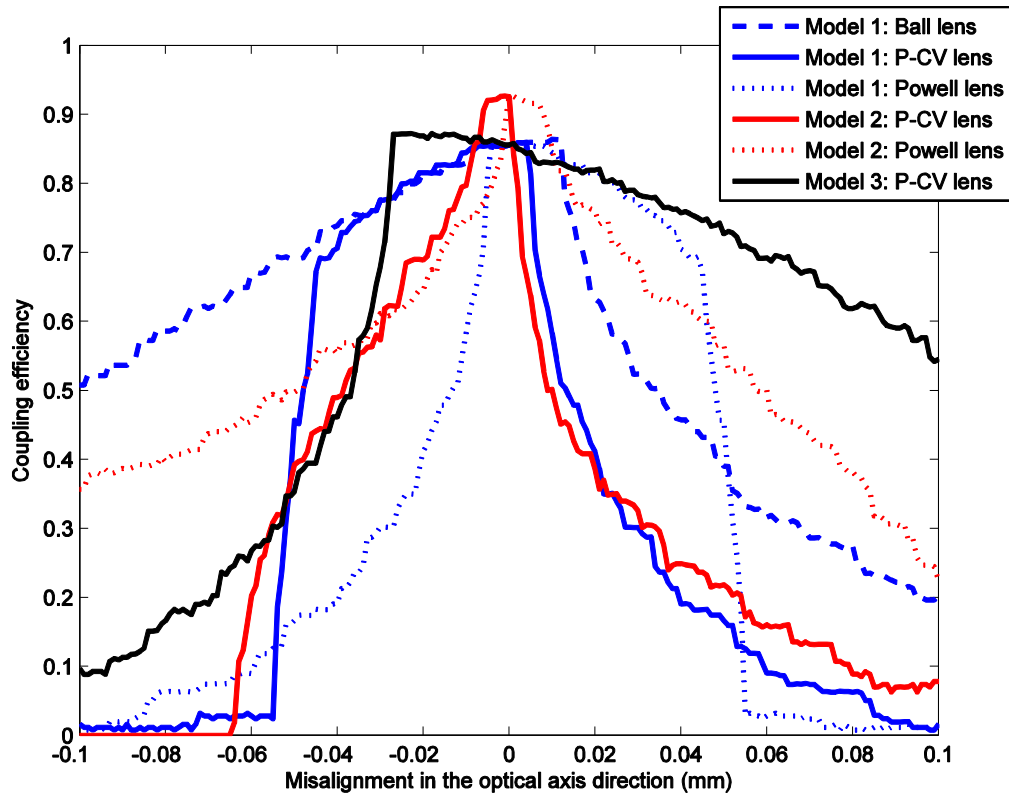


Figure 32. FRED tolerances for misalignment in the optical axis direction for all lenses separately.

In Figure 34 and Figure 35 the entire second half of the connector, the receiving connector, is displaced (see Figure 33). This is interesting since it is these two larger pieces that will be unconnected and connected to each other now and then in the field, outside the laboratory. The individual lenses are aligned in the production phase and are not supposed to move relative to each other after that. Fortunately, as can be seen in the figures, the tolerances are much higher for the receiver than for the individual lenses. In the optical axis direction the system is very stable, which is expected since the beam is supposed to be collimated between the emitter and the receiver.

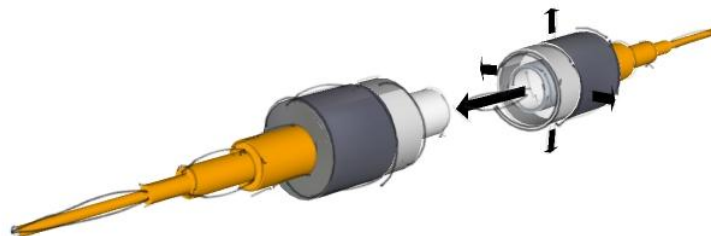


Figure 33. Illustration of the transmitting connector and the receiving connector.

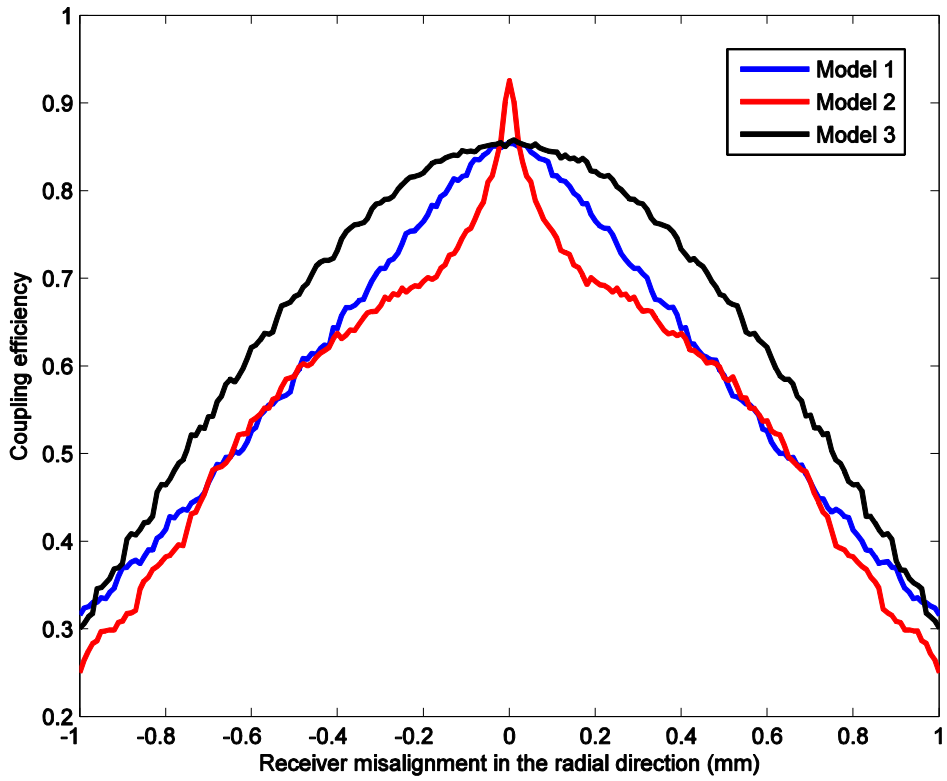


Figure 34. FRED tolerances for misalignment in the radial direction for the receiver connector.

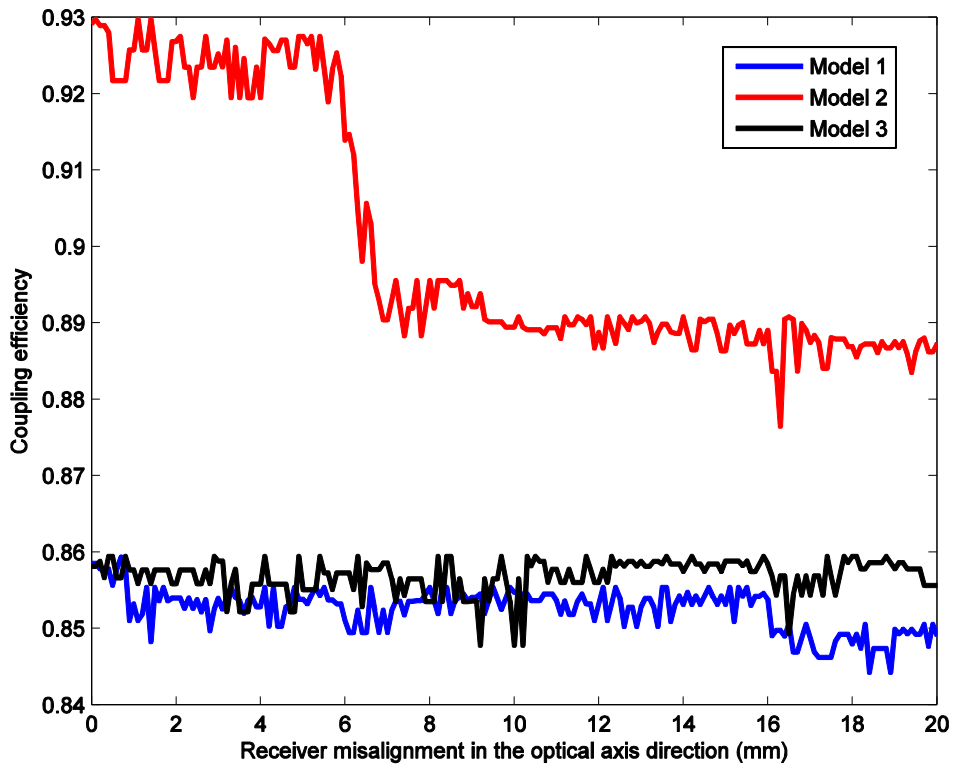


Figure 35. FRED tolerances for misalignment in the optical axis direction for the receiver connector.

At last, in Figure 36 one can see how the systems behave for wavelengths close to $1.31\ \mu\text{m}$, which the models are optimized for in this case. If $\lambda = 1.55\ \mu\text{m}$ the coupling efficiency is almost zero in this setup, but the models may as well be optimized for this wavelength.

In summary all tolerance graphs, except in this last figure, shows that the top-hat models and particularly model 2 are more sensitive for misalignments than the reference model.

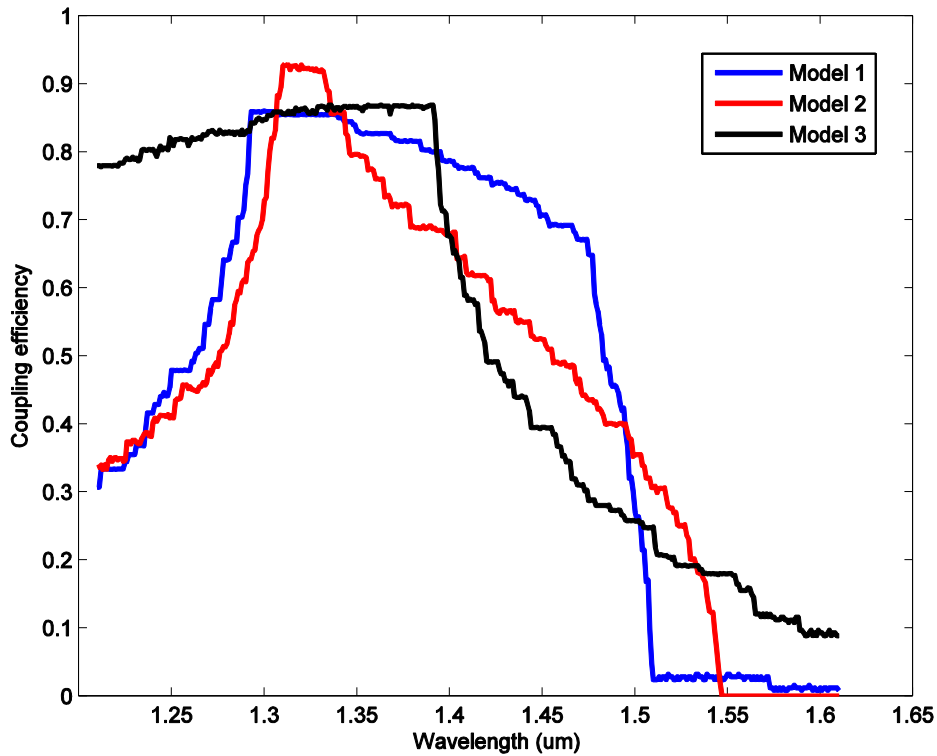


Figure 36. FRED tolerances for wavelength shift (models optimized for $1.31\ \mu\text{m}$).

5.2 Adjusted simulations for experiments

These circular symmetric Powell lenses used in the simulations are not included in any standard ranges and have to be custom made. This would be quite expensive and especially when only needed one or a few ones, because then the price of the lens includes the price of producing the tool needed for manufacturing. As an example Edmund Optics does not even accept orders of less than fifty pieces when custom made. Instead two cylindrical Powell lenses were ordered.

The first experiment performed was to analyze the transformation from Gaussian to top-hat conducted in accordance with Figure 4. Then some experiments on coupling efficiencies for single mode fiber coupling were performed. In the next section photos of the experimental setups are provided and in Figure 37 and Figure 38 the simulations

are illustrated. In the first experiment of coupling efficiency measurements, Figure 37, the setup is similar to model 3 except that the distance between the two lenses is much greater and the diameter of the expanded beam is smaller. This affect two things: The ray optics based result increases to about 98% (no reflection losses) because smaller beam diameter means less aberrations. But the POP based result decreases to about 75% because beam divergence has consequences at large propagating distances. To comment on the differences between ray optics and POP based tolerance results the receiver end (lens and fiber tip) was displaced in the transverse direction after maximum coupling efficiency was obtained. In the simulations the coupling efficiency decreased to 8% of the maximum value using ray optics and 48% of the maximum value using POP when a displacement of 1 mm was applied. The experimental measurements are discussed in the next section.

In the next stage a system combining Figure 37 and Figure 38 was simulated. The cylindrical Powell lenses were used such that in one direction the setup reminds of model 1, but in the other direction the beam is unaffected by the Powell lens and instead focused by the second lens as can be seen in the lower image in Figure 38. Here, the Gaussian beam is transformed into a uniformly illuminated line and then back again. The length of the line is much larger than the beam diameter in model 1, which increases the system aberrations. Together with the asymmetry in the transformation this resulted in a maximum coupling efficiency of just 10-20%.

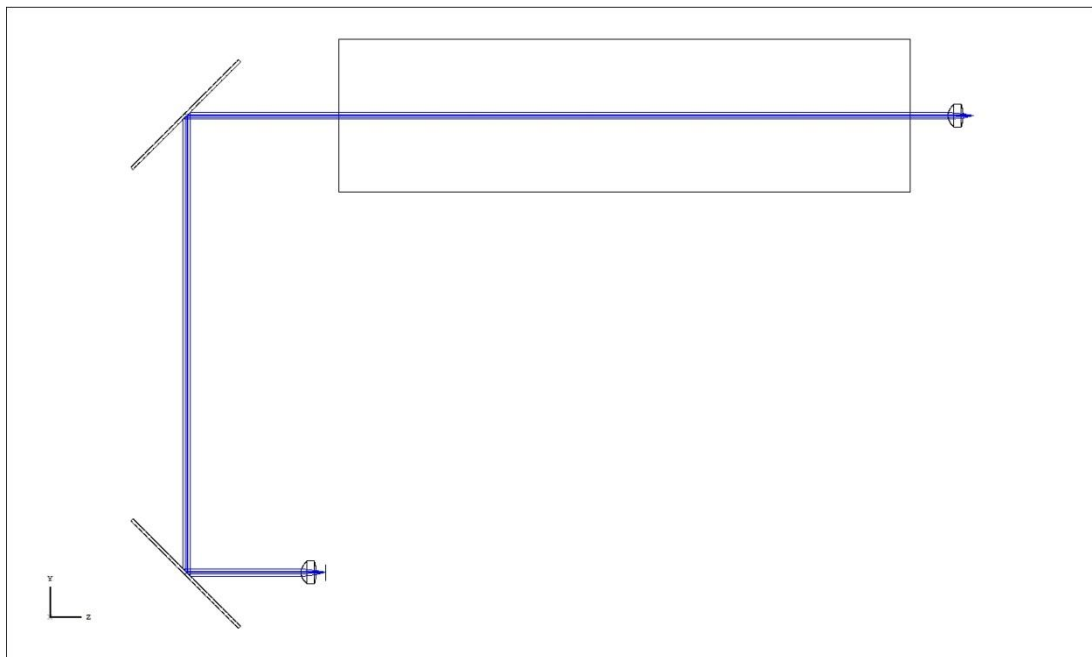


Figure 37. Simulation of fiber coupling using a collimating lens, two mirrors and a focusing lens.

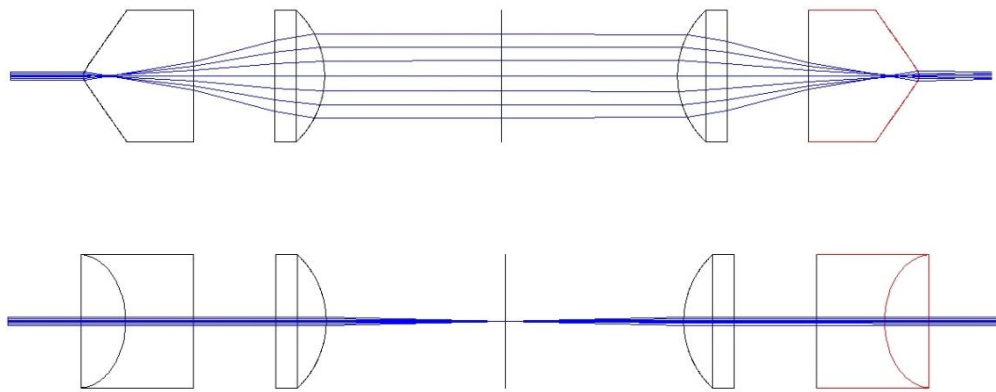


Figure 38. Optics placed in the box in Figure 37. Upper image shows y-z and lower image shows x-z.

6 Experimental results

The two cylindrical Powell lenses were placed perpendicular to each other as in Figure 4 to get a conversion from circular Gaussian to square top-hat. Unfortunately, the fan angle of these stock Powell lenses was too large, such that the diverging beam leaving the second lens was larger than the CCD-chip in the camera. Since the diverging beam has different focuses in x- and y-direction there was no easy solution to focus the beam onto the CCD-chip. Instead a He-Ne laser with visible red light was used to perform a square top-hat visible for the human eye, setup in Figure 39. No precise analysis could be done of the intensity profile, but this top-hat will not be perfect anyway since the lenses are not optimized for the laser. The objective of the experiment was to see that the conversion predicted by the theory also happens in reality and this can be seen also with the human eye or with an ordinary camera, see photos in Figure 40. One can see that the edges are much steeper for the top-hat compared to the Gaussian spot and even if the intensity distribution is not perfectly uniform, as can be seen in the photo to the left in Figure 40, it is far from being Gaussian. The bright corners in the photo are effects of too large beam diameter, since too much light hits the Powell lenses where the curvature of the lens diminishes. The profile would primarily be improved by using correct input beam diameter.

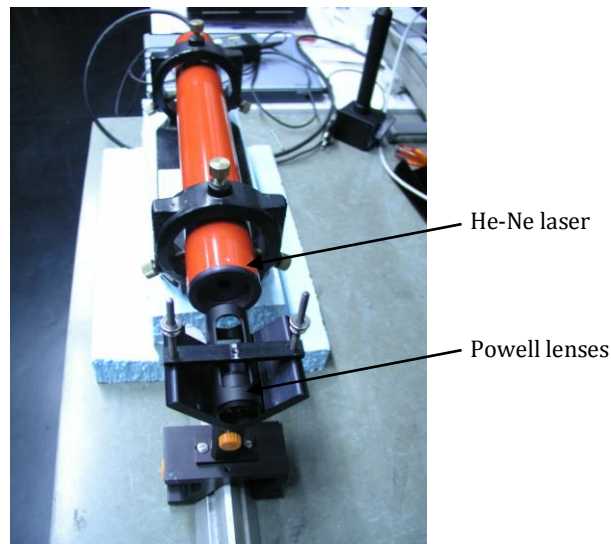


Figure 39. Photo of experimental setup for Gaussian to top-hat conversion.

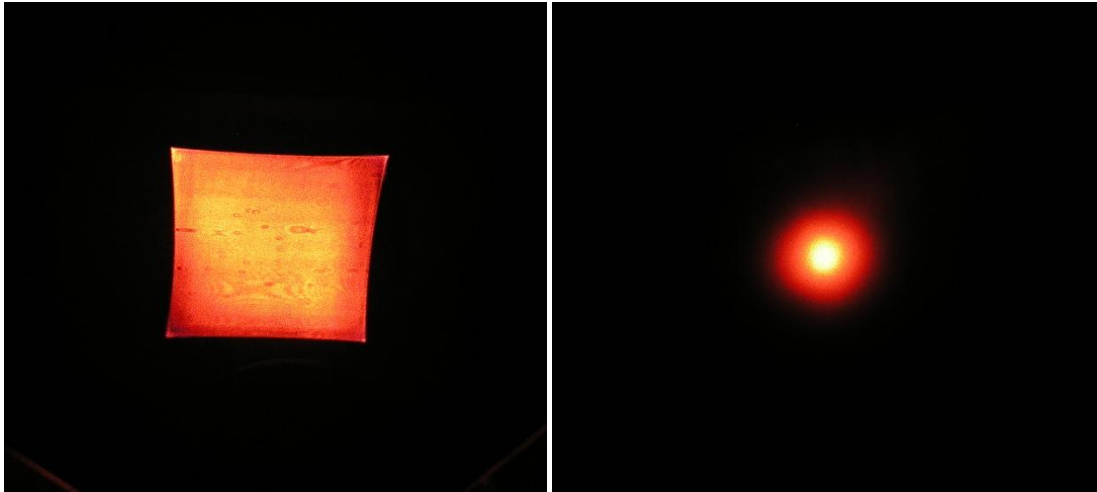


Figure 40. Photos of laser light illumination on a screen directly from laser to the right and after propagating through Powell lenses to the left.

Photos of the setups for the coupling efficiency experiments, shown illustratively in Figure 37 and Figure 38 in chapter 5.2, are provided in Figure 41. Most effort was put on the simple single-mode fiber coupling to the left in Figure 41, where just a single lens collimates the light in the emitter and an identical lens refocus the light in the receiver. Single-mode fiber coupling is not easy to achieve and very time consuming for the inexperienced user. To be feasible at all, precision instruments have to be used to adjust angles and position of the incoming beam relative to the receiving fiber. In this setup mirrors are used to correct angles and the receiving fiber is itself adjustable in the transverse directions. The collimating lenses are also adjustable in the optical axis direction relative to the fiber ends. Maximum coupling efficiency achieved in this setup was about 45%, but when shifting the transmitting fiber closer to the first mirror the coupling efficiency increased to about 74%. This is a remarkable difference which means that the coupling efficiency highly depends on the propagation length. This dependence comes from a large divergence angle that is due to a small beam diameter. In retrospect it would have been better if a collimating lens with longer focal length had been ordered such that the beam diameter would have been larger.

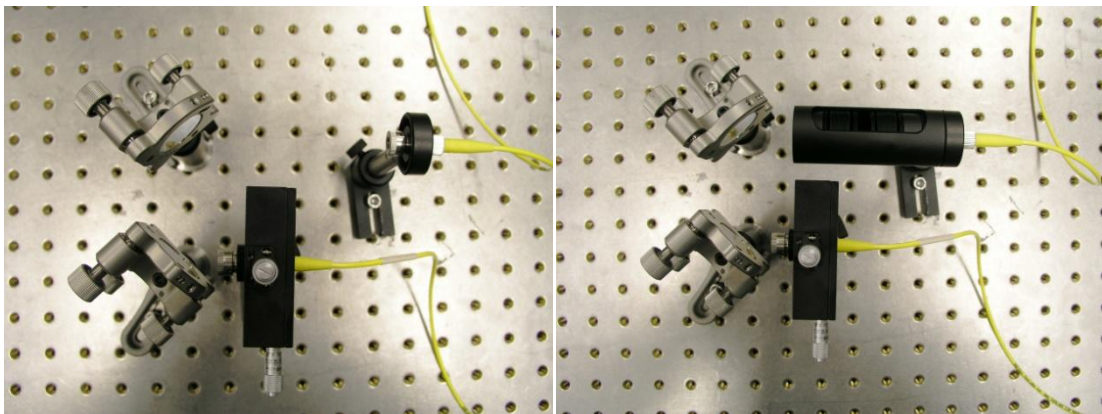


Figure 41. Photo of experimental setup illustrated in Figure 37. The tube in the right photo contains lenses illustrated in Figure 38.

The POP simulations take the beam divergence into account, but are still showing too high results (75% in the first position and about 95% when the transmitting fiber is closer to the first mirror). The reflection losses should of course be included, but this is just a few percent since the lenses are AR-coated and the mirrors have reflectivity over 99%. Still the POP simulations are much better than ray optics based simulations when having long propagation length. However, POP fails when analyzing tolerances. The experimental result of the coupling efficiency, when the receiving fiber is displaced 1 mm, is 0% and when displaced 0.5 mm it is 2.5% of the maximum value. This is even more sensitive than the simulations based on ray optics.

The experiment where the Powell lenses were used to transform the beam between the fibers can be described as unsuccessful. No coupling was achieved and the reasons are more than one. First of all, the tube used to align the lenses (right photo in Figure 41) was too imprecise, at least for the two Powell lenses, and instead the lenses should have been mounted such that they could individually be adjusted in the transverse directions. The diverging beam and small beam diameter is of course also a problem and *e.g.* in the direction not affected by the Powell lenses the beam will not be focused as in Figure 38 but rather diverge. On top of this, according to the simulations, maximum coupling efficiency of this system is just 20% even if the light would have behaved as rays. However, this experiment says very little about the original models, since the propagation length should be much shorter and the transformation less dramatic. It says though that the systems are very sensitive, which was also predicted in the tolerance section.

7 Comparison of optical simulation software FRED and ZEMAX

FRED and ZEMAX are both very powerful simulation tools and the scope of their application is wide. This project covers just a small piece of the full extent of these software and some shortcomings discussed below are maybe just applicable for this project. For other applications it could be the other way around, where the one with shortcomings here instead is superior. Of course also some general features are discussed, which should be valid in all situations.

ZEMAX is an optical design program and for lens or optical system design it is very powerful and user friendly. The work is done in a spreadsheet based 2D or 3D environment where lenses or optical systems are built up surface by surface and it is easy to define aperture stops, off axis ray bundles and so on. When having an object space, an image space, and a lens system in between, ZEMAX is very useful. The possibility of working in a sequential mode where all surfaces are ray traced in a predefined order also makes ray tracing and optimization much faster. In this thesis only the sequential mode was used, but it is also possible to work in a non-sequential mode or to have non-sequential components in an otherwise sequential system. The non-sequential mode enables *e.g.* the analysis of stray light or to use non-sequential objects or systems such as prisms and interferometers.

FRED on the other hand is an optical engineering program and is said to pick up where lens design software leaves off. Compared with ZEMAX this would best correlate with the non-sequential mode in ZEMAX and since this mode was not used in this project it is hard to say what ZEMAX is capable of. However, according to Photon Engineering [34] FRED's advantages over spreadsheet based optical design software are the following: FRED uses a 3D CAD environment which is WYSIWYG (What You See Is What You Get) and has the ability to model and analyze complete optomechanical systems. The light propagating in a 3D CAD model not only interfere with the optical elements, but also mounting and mechanical structures are taken into account. This interface is also superior when exporting the models for *e.g.* manufacturing where CAD models are needed, since spreadsheet based products are known for exporting poor CAD models. The disadvantage with using a 3D CAD environment is mainly that it is slower. In this thesis, where the sequential mode in ZEMAX is sufficient, it is more convenient to use this interface.

Another large difference between the two programs is the use of scripts. In FRED scripting (BASIC language) is a very significant part and it can be a very powerful tool in FRED. Beginners can easily learn how to make simple scripts because the help-menu is informative in this topic. In ZEMAX scripting is not as natural as in FRED and if a script is needed it is harder to understand how it should be performed. On the other hand, scripts are not needed in the same extent in ZEMAX, since the tools available in the menu system are many more and more powerful. This could be thought of as more user

friendly, but when the available tools are not good enough FRED has an advantage, as in the tolerance analysis in this thesis.

Regarding the support and help-menu both FRED and ZEMAX are good. In the help-menu tutorials and user guides are provided and in FRED also help for scripting. Both developers have knowledge bases on the internet, where in particular ZEMAX knowledge base is very helpful and rich. The FRED knowledge base is smaller, but when contacting the FRED support they responded within one day.

The optimization feature in FRED and ZEMAX is essentially the same, but it differs in how it is used. In FRED the most common optimizations are handled from the menu, but for more advanced configurations user defined scripts have to be used. In ZEMAX the optimization tool is more complete and in addition to local and global optimization routines, that are available in FRED also, something called Hammer optimization can be used. Hammer optimization does not stop if a local minimum is found but is “hammering” on until it is told not to. Some other differences and problems with the optimization were discussed in chapter 5.1.1 in the “Manually optimized top-hats” section. When comparing FRED and ZEMAX from an optimization point of view the main drawback for FRED is that there is no easy way of analyzing rays without halting them, which was discussed in that section.

Regarding correlation with experimental results one can in this thesis read that the fiber coupling calculations are a bit poor. Most problems occurs in situations where ray optics is insufficient *e.g.* at intermediate focuses and at long propagation lengths with collimated beams. The difference between the programs is insignificant when using ray optics, but ZEMAX also has the possibility of using Physical Optics Propagation (POP). However, even if POP provided better results in some situations the results did still not correlate well with the experiments done in this thesis. Furthermore it can be noticed in Figure 22 and 24–26 that ZEMAX does not offer a satisfactory image format when exporting their graphs. The solution is to export the data and plot the graphs in another program, but this is more time consuming and should not be necessary. In this report the layout differences between FRED and ZEMAX are visualized, and is the reason why these figures are not plotted in another program.

The conclusion is that ZEMAX was more suited for this project and that it is more user-friendly, which together with a good knowledge base is helpful for beginners. FRED is not far behind and for more advanced models with *e.g.* stray light analysis FRED is maybe superior. Sure is that when the available tools in ZEMAX are not enough FRED has an advantage, since scripting is a natural part of the program.

At last a short comparison of the prices. The price for ZEMAX range from \$2,500 to \$9,500 and is available in three editions, where *e.g.* the cheapest one just has access to the sequential mode. The price for FRED range from \$8,450 to \$13,950 and is available in two editions. Also notice that Photon Engineering offers discounts for use of FRED in academic research and *e.g.* for use only in this diploma project a free full version of FRED was given to the author of this report.

8 Conclusions

Gaussian to top-hat conversion of the intensity distribution is definitely possible in a single-mode fiber connector. Much research have been done on this type of transformation for other applications, and for this project a solution suitable for high transformation efficiency and limited space has been chosen. The Powell lens will transform the beam into a top-hat, but the main difficulty is to couple the light into the next fiber, which requires a good retransformation to a Gaussian intensity profile. Each lens introduces aberrations and contributes to an imperfect Gaussian profile at the receiving fiber end. To predict the coupling efficiencies reliable simulation tools are needed, but in this thesis it has been seen that the predicted coupling efficiencies could be wrong and here we mainly have to realize the limitations of ray optics. For a small beam diameter ray optics can be inaccurate, especially when propagating as a collimated beam or having intermediate focuses. At the end of this diploma work it was thought of using concave Powell lenses instead of convex, which would remove the intermediate focuses. It should also be said that the propagation lengths in a fiber connector are much shorter than in the experiments in this project and my analysis is that the simulations of model 1 (Figure 16, p. 26) are close to reality. At least we could analyze the simulations compared to the simulations from the reference model, and see that compared to a random expanded beam fiber connector the two models in this thesis are equally good regarding coupling efficiency, but more sensitive for misalignments.

To further develop this product, real experiments on the actual models should be done. The main barrier is to finance the components of the prototype, but when one lens is manufactured it will not be that expensive to fabricate this lens in large volumes.

Regarding the comparison between FRED and ZEMAX these two simulation tools are to a large extent equally good. Their primarily focus differ somewhat and the programs are better/worse in different areas. However, in this thesis ZEMAX is preferred.

9 Acknowledgments

I would like to thank my supervisors Per Olof Hedekvist and Johan Mauritsson for all your support. Thanks Per Olof for introducing me to this diploma work, it has been very interesting and I have learned a lot. Even if the experiments were not as successful as I hoped for it has been a great learning experience to me and it was educational to go through all steps for the experiments, from designing a setup to order all components and finally perform the experiments, mainly on my own. I would also like to thank all my colleagues at SP and particularly Anne Andersson for introducing me to the fiber lab. But my greatest thanks to Martin Zelan for many interesting discussions and guidance in the fiber lab.

References

- [1] H. M. Presby, A. Benner and N. Amitay, "Research on an expanded beam single-mode fiber-optic connector," *Applied Optics*, vol. 27, no. 15, pp. 3121-3123, 1988.
- [2] P. W. Rhodes and D. L. Shealy, "Refractive optical systems for irradiance redistribution of collimated radiation: their design and analysis," *Applied Optics*, vol. 19, no. 20, pp. 3545-3553, 1980.
- [3] C. C. Aleksoff, K. K. Ellis and B. D. Neagle, "Holographic conversion of a Gaussian beam to a near-field uniform beam," *Optical Engineering*, vol. 30, no. 5, pp. 537-543, 1991.
- [4] C. Y. Han, Y. Ishii and K. Murata, "Reshaping collimated laser beams with Gaussian profile to uniform profiles," *Applied Optics*, vol. 22, no. 22, pp. 3644-3647, 1983.
- [5] D. Palima and J. Glückstad, "Gaussian to uniform intensity shaper based on generalized phase contrast," *Optics Express*, vol. 16, no. 3, pp. 1507-1516, 2008.
- [6] F. M. Dickey and S. C. Holswade, "Gaussian laser beam profile shaping," *Optical Engineering*, vol. 35, no. 11, pp. 3285-3295, 1996.
- [7] Edmund Optics, [Online]. Available: <http://www.edmundoptics.com/optics/optical-lenses/aspheric-lenses/plano-convex-pcx-axicons/3364>. [Accessed 4 September 2012].
- [8] Laserline Optics Canada Inc., [Online]. Available: http://laserlineoptics.com/6mm_powell_lens.html. [Accessed 4 September 2012].
- [9] K. Aït-Ameur and F. Sanchez, "Gaussian beam conversion using an axicon," *Journal of Modern Optics*, vol. 46, no. 10, pp. 1537-1548, 1999.
- [10] A. E. Martirosyan, "Transformation and measurement of parameters of gaussian, laguerre-gaussian, and super-gaussian beams by using a light filter based on absorbing axicon," *Journal of Contemporary Physics (Armenian Academy of Sciences)*, vol. 46, no. 5, pp. 211-217, 2011.
- [11] Y. Kawamura, Y. Itagaki, K. Toyoda and S. Namba, "A simple optical device for generating square flat-top intensity irradiation from a gaussian laser beam," *Optics Communications*, vol. 48, no. 1, pp. 44-46, 1983.
- [12] Coherent Inc., "Efficient Transformation of Gaussian Beams into Uniform, Rectangular Intensity Distributions," White Paper. [Online]. Available: <http://www.coherent.com/Ads/?fuseaction=Forms.page&PageID=748>. [Accessed 4

September 2012].

- [13] F. Cayer, "Rectangular flat-top beam shaper". US Patent US7400457 (B1), 15 July 2008.
- [14] O. Homburg and T. Mitra, "Gaussian-to-top-hat beam shaping: an overview of parameters, methods, and applications," in *SPIE Proceedings*, Dortmund, 2012.
- [15] J. P. Girardeau-Montaut, J. C. Li and C. Girardeau-Montaut, "Optical device analysis for uniform intensity irradiation from a high energy gaussian laser beam," *Optics Communications*, vol. 57, no. 3, pp. 161-165, 1986.
- [16] L. Frantzych, "Implementation of optical simulations for product development at the division of optoelectronics, Sony Ericsson Mobile Communications AB," Lund Reports on Atomic Physics, LRAP-425, Lund University, 2010.
- [17] Optenso, "Links on Optical Design and Engineering," [Online]. Available: <http://www.optenso.com/links/links.html>. [Accessed 30 September 2012].
- [18] B. E. A. Saleh and M. C. Teich, *Fundamentals of Photonics*, New Jersey: John Wiley & Sons, Inc., 2007.
- [19] E. Hecht, *Optics* (4th edition), San Francisco: Pearson Education, Inc., 2002.
- [20] I. Powell, "Linear deiverging lens". US Patent US4826299 (A), 2 May 1989.
- [21] A. S. Glassner (Ed.), *An Introduction to Ray Tracing*, San Francisco: Morgan Kaufmann Publishers, Inc., 1989.
- [22] Edmund Optics, "About Us," [Online]. Available: <http://www.edmundoptics.com/company/history/about-us/?ref=menu>. [Accessed 30 October 2012].
- [23] CVI Melles Griot, "About Us," [Online]. Available: <https://www.cvimellesgriot.com/Company/AboutUs.aspx>. [Accessed 30 October 2012].
- [24] JML Optical, "About Us," [Online]. Available: <http://www.jmloptical.com/about-us/>. [Accessed 30 October 2012].
- [25] Newport Corporation, "Company Overview," [Online]. Available: <http://www.newport.com/cms/company/company-overview>. [Accessed 30 October 2012].
- [26] OptoSigma, "About OptoSigma," [Online]. Available: <http://www.optosigma.com/company>. [Accessed 31 October 2012].
- [27] Rolyn Optics, "Rolyn Optics Company History," [Online]. Available:

- http://www.rolyn.com/rolyn_history/rolyn_history.htm. [Accessed 31 October 2012].
- [28] Thorlabs, [Online]. Available: http://www.thorlabs.com/about_us.cfm. [Accessed 31 October 2012].
- [29] Asphericon, "Your expert in aspheres," [Online]. Available: <http://www.asphericon.net/en/unternehmen/kernkompetenz>. [Accessed 15 November 2012].
- [30] Zemax Development Corporation, ZEMAX User's Guide, 2006.
- [31] E. Hewitt and R. E. Hewitt, "The Gibbs-Wilbraham phenomenon: An episode in fourier analysis," *Archive for History of Exact Sciences*, vol. 21, no. 2, pp. 129-160, 1979.
- [32] Photon Engineering, "Optimizing for a Target Distribution," [Online]. Available: <http://fred-kb.photonengr.com/2010/12/14/optimizing-for-a-target-distribution/>. [Accessed 15 January 2013].
- [33] N.-H. Kim, "How to Design a Gaussian to Top-Hat Beam Shaper," 4 October 2006. [Online]. Available: <http://www.radiantzemax.com/kb-en/Knowledgebase/How-to-Design-a-Gaussian-to-Top-Hat-Beam-Shaper?Keywords=gaussian+top-hat>. [Accessed 26 November 2012].
- [34] Photon Engineering, [Online]. Available: <http://www.photonengr.com/software/faq/>. [Accessed 5 December 2012].
- [35] GigaCom AB, "About us," [Online]. Available: <http://www.gigacom.se/content.php?cid=1>. [Accessed 31 August 2012].